1971

Vibrational relaxation of anharmonic oscillators

Lowell Dean McMillen
Iowa State University

Vibrational relaxation of anharmonic oscillators

by

Lowell Dean McMillen

A Dissertation Submitted to the

Graduate Faculty in Partial Fulfillment of

The Requirements for the Degree of

DOCTOR OF PHILOSOPHY

Major Subjects: Aerospace Engineering
Mechanical Engineering

Approved:

Signature was redacted for privacy.

In Charge of Major Work

Signature was redacted for privacy.

For the Major Departments

Signature was redacted for privacy.

For the Graduate College

Iowa State University
Ames, Iowa

1971

TABLE OF CONTENTS

LIST OF SYMBOLS

A_i = Jacobian matrix of $\underline{F}$

$a_{\ell k}$ = element of matrix A_i

a' = empirical constant in Equation 2.1

d_e = dissociation energy of oscillator

E_d = energy defect defined by Equation 2.7

E_r = vibrational energy of rth oscillator level

$E_V(t)$ = vibrational energy at time t

$\bar{E}_V(t)$ = $E_V(t)/h\nu$, non-dimensional vibrational energy

$\underline{F}$ = vector whose elements are the right hand side of master relaxation equations

$\underline{f}_i$ = vector whose elements are the linear terms of $\underline{F}$ at some reference step

H = stepsize

h = Plank's constant

$\hbar$ = $h/2\pi$

K = uppermost quantum level

°K = degrees Kelvin

k = Boltzmann constant

L = range of repulsive forces

ℓ' = $L/2\pi$

ℓn = logarithm to base e

Log = logarithm to base 10

m = mass of oscillator

n = total number of heat bath oscillators

n_r = fraction of oscillators in level r

$\hat{n}_r$ = population of oscillators in energy level r

$\underline{n}$ = vector whose elements are n_r's

P_{mr} = thermally averaged vibration-translation transition probability

$P_{s,r;\ell,m}$ = thermally averaged vibration-vibration transition probabilities

$\hat{P}_{s,r;\ell,m}$ = vibration-vibration transition probability per collision

P'_{sr} = vibration-translation transition probabilities defined by Equation 2.17

p = pressure

R = reduced vibrational energy

r = quantum number

r' = instantaneous separation distance

r'_e = equilibrium separation distance

T = temperature of heat bath and translational temperature

T_V = vibrational temperature

T_r = vibrational temperature of a quantum level

T_c = $h\nu/k$, characteristic vibrational temperature

t = time

t' = $P_{10}nt$, nondimensional time

U_{rm} = harmonic oscillator matrix elements

$\bar{V}$ = average number of vibrational quanta defined by Equation 2.23

V-T = vibration-translation

V-V = vibration-vibration

v_o = translational velocity of oscillators

X = Morse potential function

Z = number of collisions per unit time suffered by an oscillator when the gas density is one oscillator per unit volume

ε = normalizing or ordering parameter defined by Equation 2.17

γ = parameter defined in Equation 2.21

μ = reduced mass of oscillator

Φ = parameter in Equation 2.18

ϕ = τ_{sho}/τ_{aho}

θ_1^* = population factor or vibrational temperature of the first vibrational level

ν = vibrational frequency for lowest vibrational state

τ = vibrational relaxation time

τ_{VV} = time scale for vibration-vibration collisional processes

τ_{VT} = time scale for vibration-translation collisional process

ω_e = anharmonicity of anharmonic oscillator

Subscripts

aho = denotes anharmonic oscillator

i = reference step in a discrete variable algorithm

ℓ,m,r,s = integer denoting vibrational quantum numbers or levels

sho = denotes simple harmonic oscillator

Superscripts

(0) = denotes zeroth order

(1) = denotes first order

CHAPTER I. INTRODUCTION

Opening Statements

The development of theories to explain the real gas phenomenon of vibrational energy relaxation is certainly not new and until recently most of the theoretical and experimental works concerned with vibrational relaxation agreed in their findings. Recently, there have been some discrepancies between vibrational relaxation times measured in shock tube experiments and those measured in expansion flow experiments. It has been found that de-excitation rates during rapid expansion are from one to three orders of magnitude faster than for excitation rates. An explanation and study of these discrepancies has been done by others (5-7, 16, 17, 46) by using anharmonic oscillator theory instead of harmonic oscillator theory to model the individual vibrating molecules in a vibrational, de-excited gas. Also, much interest in vibrational energy transfer between molecules is being generated as a result of gasdynamics laser studies (4, 12, 13).

This dissertation is the theoretical investigation of vibrational energy relaxation and vibrational level population changes for a pure diatomic gas using anharmonic oscillator theory in a simulated expansion flow environment. The motivation for this research was to extend the research of Treanor, Rich and Rehm (46), Bray (6) and Hsu and Maillie (16,

17) for the de-excitation problem in a more complete manner by the numerical integration of the complete master relaxation equations. In no way is the previous statement meant to convey that this dissertation represents a completion of a research area, but rather this dissertation increases the understanding of the vibrational relaxation process in an expansion flow and hopefully, will be an impetus for more research on the vibrational energy relaxation problems to be discussed in this work.

The remainder of this chapter will be devoted to a literature review followed by a more concise statement of the research problem and objectives of this dissertation.

Summary of the Literature Review

Historically, much of the reported research concerned with energy exchange or transfer to and from the vibrational degree of freedom has treated this energy exchange process as a collisional process between two molecules or species. Two basic exchange processes have been studied. One of these processes has been referred to, and will continue to be, as vibrational-translational or V-T energy exchange. In a V-T energy exchange one of the colliding molecules gains or loses quanta of vibrational energy while the colliding partner loses or gains the equivalent amount of translational energy. The other exchange process is the vibration-vibration (V-V) energy

exchange when two molecules or oscillators collide. Quite simply, in a V-V energy exchange process one oscillator gains or loses quanta of vibrational energy and the colliding partner loses or gains these quanta of energy. For simple harmonic oscillator theory the previous statement is an accurate description of the V-V exchange process. For anharmonic oscillator theory, the translational energy mode will also be a factor in the V-V exchange process. More discussion of this point will be given in Chapter II.

Vibrational energy exchange processes for diatomic gases are a high temperature phenomenon (8, 48) and are of interest to the gas dynamist and to the physical chemists. For the gas dynamist vibrational energy relaxation is of concern whenever the characteristic vibrational relaxation time and the characteristic flow time are of the same order. As explained by Cottrell and McCoubrey (9), vibrational energy exchange studies are essential to the understanding of reaction kinetics by the physical chemists.

Probably the most famous early works treating vibrational energy relaxation were the two due to Landau and Teller (20) in 1936 and Bethe and Teller (2) in 1940. A remarkably simple equation describing the relaxation of vibrational energy in the absence of dissociation has been attributed to both sets of authors and is (2)

$$\frac{dE_V(t)}{dt} = \frac{E_V(\infty) - E_V(t)}{\tau(p,T)} \tag{1.1}$$

where $E_V(t)$ is the vibrational energy at time t, $E_V(\infty)$ is the vibrational energy at equilibrium and $\tau(p,T)$ is the characteristic vibrational relaxation time at the local pressure and temperature. Equation 1.1 was derived from a set of rate equations which describe how each vibrational energy quantum level is populated and depopulated by quantum transitions. Imbedded in the Bethe-Teller equation (or Landau-Teller) are the following conditions: (1) the energy levels are equally spaced which is a result of using harmonic oscillators as a model for the gas molecules; (2) vibrational collisional transition rates are of the Landau-Teller form (20)

$$P_{r+1,r} = (r+1)P_{1,0} \tag{1.2}$$

where $P_{r+1,r}$ is the probability of transition from quantum level r+1 to quantum level r and $P_{1,0}$ is the probability from level 1 to level 0; and (3) vibrational transitions occur stepwise from one vibrational level to the next adjacent level (single quantum jumps). This equation has been used extensively in fluid flow problems involving vibrational energy relaxation and in the evaluation of experimental relaxation times for vibrational energy. Although Equation 1.1 has proved to be quite successful, it is a macroscopic equation

and therefore hides the intrinsic behavior of the individual quantum levels.

Equations 1.1 and 1.2, taken generally, describe or reflect the two basic problem areas that have been studied theoretically in the area of vibrational relaxation of a gas (45). One is the determination of the transition probability that a molecule will change vibrational states. The second is the use of these transition probability results to determine the population of molecules in various vibrational levels. This latter study requires the solution of a set of rate equations. It is the first moment of these rate equations for harmonic oscillators (2) that results in Equation 1.1. An excellent review of the research done prior to 1969 in evaluating transition probabilities using various theoretical models is given by Rapp and Kassal (35).

Rubin and Shuler (37) used the above conditions listed for the Bethe-Teller equation in studying the relaxation of vibrational level distributions of a small number of excited diatomic molecules immersed in an inert constant temperature heat bath. In this paper, they noted that an initial Boltzmann distribution relaxes to a final Boltzmann distribution via a sequence of Boltzmann distributions, thereby allowing the defining of a vibrational temperature that is time dependent. In a second paper, Rubin and Shuler (38) showed that if the transition probabilities vary in an exponential manner with

increasing quantum number the intermediate Boltzmann distributions were not obtained. Although the above solutions were obtained numerically or approximately, Montroll and Shuler (28) obtained exact solutions to the problem of Reference 37. Another important result of the above studies was that for harmonic oscillator theory, the vibrational energy relaxation process (Equation 1.1) is independent of the population distribution.

Even when the collisional model was changed to allow for collisions which permitted V-V energy exchanges, Shuler (43) and Osipov (31) concluded that an intermediate Boltzmann distribution will prevail during a relaxation process for the conditions listed after Equation 1.1. A Boltzmann distribution throughout the relaxation process is a result of the harmonic oscillator model (32).

As explained by Osipov and Stupochenko (32), the use of harmonic oscillator theory and Equation 1.1 has proved to be quite successful for problems in which the lower vibrational levels play the predominate role, for example in gas behavior behind a shock wave. However, such is not the case for situations in which upper quantum levels can be of importance as will be discussed below.

In 1964 Hurle, Russo and Hall (19) reported that relaxation times for expansion flow environments (vibrational de-excitation) were much shorter than for shock tube studies when

nitrogen was the gas being studied. Other experimentalists (3, 18, 39, 49, 50) have obtained similar results for nitrogen (18, 39) and carbon monoxide (3, 49, 50). Impurity considerations certainly cannot be neglected (39, 49, 50) but to what extent is not certain. It must be mentioned here that there has been a large variation as to what is the magnitude of the enhanced relaxation rate. The numbers vary all the way from 1 to the order of 10^3 (7); however, it appears that as a result of more exact and precise experimental procedures available in the late 60's, the enhancement is not as much as was found in 1964 (50). A possible cause for this variation will be given later in Chapter III.

As stated earlier, the anharmonic oscillator studies of Treanor et al. (46) and Bray (5-7) were put forth to explain the above anomalies because in theory it is expected that the same relaxation rate would exist for a given temperature and pressure for both excitation and de-excitation on the basis of harmonic oscillator theory for vibrational energy relaxation. Anharmonic oscillator models (8) for a diatomic gas molecule causes the energy level spacings to decrease as the quantum number is increased. Furthermore, the transition probabilities for V-T exchange processes no longer obey the linear relationship of the Landau-Teller form. In fact, because of the anharmonicity the transition probabilities increase more rapidly for the anharmonic oscillators than the harmonic

oscillators. Bazely et al. (1) using anharmonic oscillators relaxing in an inert constant temperature heat bath found that significant deviations from the Boltzmann distribution do not occur at lower levels with the difference being the order of the anharmonicity when the initial distribution is Boltzmann. For their investigation, Bazely et al. (1) considered only V-T exchange processes in the collision dynamics.

In the anharmonic model studies of Treanor et al. (46), Bray (5-7), Fisher and Kummler (11) and Hsu and Maillie (16, 17) where vibrational de-excitation is considered both V-T and V-V energy exchange processes were considered. For temperatures well below the characteristic vibrational temperature of a diatomic gas the energy exchange processes are dominated (i.e., V-V transition probabilities are much larger than V-T transition probabilities) by the V-V exchange processes at the lower vibrational levels (36, 46). Treanor et al. (46) in an isothermal heat bath case restrict their anharmonic model to the regime of vibrational quantum numbers where V-V exchange domination is assured. They show that for this V-V dominated model the energy relaxation can be separated into two separate time scales. When the system is initially disturbed from equilibrium, in a very short time scale the rapid V-V exchange mechanism assures a quasisteady distribution of the molecules. On a very much longer time scale the vibrational energy is brought into final equilibrium with the low temperature

translational energy mode by the slower V-T exchange processes while the quasisteady distribution is being maintained by the V-V exchange processes.

The mathematical technique employed by Treanor et al. (46) was a Chapman-Enskog procedure whereby the terms of the population rate equations (master relaxation equations) are ordered according to the rates of the vibrational energy exchange (V-T and V-V exchanges). They arrive at an expression for the quasisteady distribution which is definitely a non-Boltzmann distribution by ignoring the transient period between initial nonequilibrium and the quasisteady state time (this time corresponds to the length of the short time scale mentioned above). This Treanor distribution will eventually reach a Boltzmann distribution when final equilibrium is reached but the intermediate distributions will be of the Treanor form. For a system of harmonic oscillators where V-V and V-T exchange mechanisms are present, it has been found (31, 33, 40) that the quasisteady distribution is Boltzmann. The relaxation of the first moment equation was also investigated by Treanor et al. (46). By this analysis they were able to show an enhancement of the energy relaxation rate over that of the Landau-Teller model for situations where initially high vibrational energy is coupled with low translational temperature. These relaxation rates are calculated at a time corresponding to the initial quasisteady state. The enhanced

relaxation rates are related to the inversions occurring in the population distributions. As conjectured by Treanor et al. (46) and shown by Bray (6) the upper level reversals may not be very large, and in fact, as the quantum number increases the molecular population reaches a peak and then will follow a distribution for the uppermost levels in an anharmonic model that is close to a Boltzmann distribution consistent with the translational temperature.

Bray (6) analyzes the vibrational energy de-excitation problem using an anharmonic model under isothermal heat bath conditions. Bray's model also includes both V-T and V-V exchange processes; however, he has no restrictions on the levels used as did Treanor et al. (46). Therefore, his model cannot be termed V-V dominated or even V-T dominated. Bray (6) obtains what he calls a full solution to the master relaxation equations by using the master relaxation equations and a first moment equation to iterate on an initial Treanor distribution. He assumes sufficient time has elapsed so that a quasisteady distribution (Treanor distribution) can be found before he calculates his full solution. His full solutions show that the lower level populations (where V-T rates << V-V rates) follow a Treanor distribution form and the upper levels (V-T rates > V-V rates) approach a Boltzmann form consistent with the translational temperature. The intermediate levels are a transition region between the lower Treanor distribution and the upper Boltzmann distribution and therefore will exhibit

a peak in the distribution. Bray (6) investigated energy relaxation of his full solution by comparing temperature relaxation rates between the full solution and the Landau-Teller rate and showed an enhancement of the anharmonic model relaxation rate due to the V-V energy exchange and anharmonicity. The results are calculated at some initial quasisteady state.

Bray also analyzed flow situations (7) where the restriction of isothermal heat bath is removed for CO gas. He showed distortion of vibrational population distribution due to a prescribed temperature gradient can give the appearance of an enhanced de-excitation rate although there is no removal of vibrational quanta from the system. Again, his work is reported at a specified quasisteady state.

In Hsu and Maillie's reported research (16, 17), they estimated the order of magnitude for the vibrational energy de-excitation rate as a function of nondimensional time using a V-V dominated model analysis and V-T dominated model analysis of the expansion flow problem. The V-V dominated model is essentially the Treanor et al. (46) model where the first moment equation is integrated with respect to a time parameter. The V-T dominated model is an integration of the master relaxation equations with the V-V terms set equal to zero. This V-T dominated solution begins at quasiequilibrium, or the initial quasisteady state corresponding to the Treanor et al. (46)

solution, with an initial Treanor distribution. Again there is a truncation of levels used and time solutions begin from a quasisteady state. The V-T dominated model of Hsu and Maillie was used mainly for comparison purposes and may serve as an error measurement for the V-V dominated model. Although the V-T dominated model arrived at population distribution that differed radically from the V-V dominated model, the relaxation rates were surprisingly close in magnitude. Further, the factor relating the vibrational energy relaxation time of the Landau-Teller model with their models was stated at most to be a factor of 5 near initial quasiequilibrium and quickly falling to a value less than two in a very short time (17). This is in agreement with recent experimental work (3, 50).

The Research Objective

As can be seen by the above discussion and to the author's knowledge no attempt has been made to solve the master relaxation equations from initial nonequilibrium using all the terms in the master relaxation equation for an anharmonic oscillator throughout the time process. This will be done for a simulated expansion flow environment. This approach is not a first moment approach as described above for calculating the relaxation rates, and no a priori population distribution form is needed to arrive at a solution as in the above studies.

This more complete solution and its results can serve as a comparative model to the above mentioned models (6, 17, 46) in evaluating their strengths and weaknesses.

Time variations of relaxation rates for vibrational energy and population "temperatures" will be calculated and compared with corresponding Landau-Teller rates. As was stated by Hsu and Maillie (16, 17) and will be shown here the relaxation rates for the anharmonic model and harmonic model only differ by any appreciable magnitude only in the early stages of the relaxation process or in the time regime corresponding to the initial quasisteady state used by Treanor et al. (46), Bray (5-7) and Hsu and Maillie (16, 17). Because of the large computational time required to integrate large quantum level cases, these solutions will be terminated at times when the relaxation rates are very small or when the rates are approximately the same magnitude as those for harmonic oscillator theory.

By using different truncated anharmonic models, it will be shown that the full or nearly full level anharmonic model is only important in the early stages of relaxation in calculating relaxation rates. Because it was shown in Reference 7 that for nitrogen it takes extremely large temperature gradients (certainly not unrealistic) for non-isothermal heat bath to be important, this research will continue to use the isothermal heat bath conditions used by previous investigators (5, 6, 17, 46).

CHAPTER II. THEORETICAL TREATMENT

Introductory Remarks

In this chapter the master relaxation equations for vibrational relaxation of a diatomic gas using anharmonic oscillator models for the molecules will be developed. This form will be consistent with the conditions of the physical model described in the next section. The master relaxation equations for vibrational relaxation are a set of differential equations that are derived from a more general set of rate equations which describe the rate at which the population of a given vibrational quantum level is changing with respect to time. These general rate equations allow for multiple quantum exchanges of energy by various collisional processes, dissociation effects, recombination and radiation.

Because this research is based on the research of Treanor et al. (46), Bray (6) and Hsu and Maillie (17), the molecular model and its environment to simulate an expansion flow process is based on these references (There are some notational differences, but the majority of the notation is that of Treanor et al. (46).). A more thorough discussion of the above authors' research will be presented to show primarily the improvement of the present analysis when compared to these theories.

Also, in this chapter will be a discussion of the numerical techniques employed to solve the set of master relaxation equations with the comments and discussion tempered by the author's readings of Lomax and associates (22-25) and Magnus and Schechter (26).

The Physical Model

The following model was employed to study the vibrational relaxation of a diatomic gas in an expansion flow environment.

1. A system of excited diatomic anharmonic oscillators initially at high temperature are immersed in a diluent heat bath of similar oscillators at a lower temperature. An isothermal condition on the heat bath temperature is imposed throughout the relaxation process.

2. Excited oscillators exchange vibrational energy with both the translational and vibrational modes of the heat bath oscillators.

3. No dissociation, recombination or radiation is permitted. Energy exchange is accomplished by collision only.

4. The molecules are treated as Morse anharmonic oscillators which have a potential energy given by (8)

$$X = d_e(1 - e^{-a'(r'-r_e')})^2 \qquad (2.1)$$

where d_e and a' are empirical constants related to the dissociation energy and vibrational frequency of the lowest

state, r' and r_e' are respectively, the instantaneous separation distance and equilibrium separation distance between the two molecules of the oscillator.

5. Single quantum jumps only are permitted. For translational temperatures below the characteristic vibrational temperature single quantum jumps are much more likely than multiple quantum jumps for both the V-V energy exchange (46) and T-V energy exchange (30) processes.

6. A one dimensional collisional model is assumed for both the T-V and V-V transition probability calculations.

With a potential energy function of the above form (Eq. 2.1), solution of the Schrödinger wave equation permits the following energy levels (8)

$$E_r = (r - \omega_e r^2) h \nu \qquad (2.2)$$

where r is the vibrational quantum level or number, h is Plank's constant, ν is the fundamental frequency of the lowest vibrational state and ω_e is the anharmonicity of the molecule and is given by

$$\omega_e = h\nu/4d_e \qquad (2.3)$$

Furthermore, the number of energy levels allowed for a given diatomic molecule is dependent on the dissociation energy and fundamental frequency of that molecule.

Master Relaxation Equations

The basic kinetic equation that describes the time rate of change of the number of molecules per cm^3 in each quantum level is governed by conservation equations of the form

$$\frac{d\hat{n}_r}{dt} = \sum_{m=0}^{K} (P_{mr}\, \hat{n}_r\, n - P_{rm}\, \hat{n}_r\, n) + \sum_{m=0}^{K} \left[\sum_{\ell \neq s}^{K} \sum_{s=0}^{K} P_{\ell,m;s,r} \hat{n}_r \hat{n} - P_{s,r;\ell,m} \hat{n}_r \hat{n}_s \right] \quad r = 0,1,2,\ldots,K \qquad (2.4)$$

In Equation 2.4, $\hat{n}_r$ is the concentration of molecules in the r-th vibrational level; K is the uppermost bound vibrational level; n is the total number concentration of molecules. P_{mr} is the V-T exchange rate constant for the collisional exchange process

$$\hat{n}_m + n \rightarrow \hat{n}_r + n \qquad (2.5)$$

where the vibrational energy representing the difference between the m-th and r-th quantum level is transferred to or from the translational mode of the heat bath oscillators. $P_{m,\ell;r,s}$ is one of the V-V exchange rate constants for the collisional process

$$\hat{n}_m + \hat{n}_\ell \rightarrow \hat{n}_r + \hat{n}_s \qquad (2.6)$$

in which vibrational energy is exchanged with the translational mode due to an energy defect given by

$$E_d = (E_m - E_r) - (E_s - E_\ell) \qquad (2.7)$$

The energy given by Equation 2.7 is transferred into the translational mode if its sign is negative and from the translational mode if the sign is positive. Furthermore, the V-V exchange rates can be of two kinds. One is when equal numbers are exchanged within the vibrational mode for the V-V collisional process, that is, m-r = s-ℓ. Therefore, there is a conservation of quanta during the exchange process; however, for anharmonic oscillator interactions there will in general not be a conservation of vibrational energy. In situations where there is no exchange of vibrational energy with the translational mode a condition exists which is termed resonance. For harmonic oscillators all exchanges are resonance when conservation of quanta exists. The other kind of exchange is when there are some quanta exchanged with the translational mode as well as the vibrational mode so that $m-r \neq \ell-s$. However, as a result of the large resonance defect during these exchanges, these "uneven exchange" rates are not only smaller than the V-V rates associated with the "even" exchange of vibrational quanta but are also much smaller than

the direct V-T exchange rates (36). Therefore, only V-V exchange processes in which there is a conservation of the number of quanta are permitted; and in addition, because of condition 5 of the physical model only single level jumps will be allowed in these exchanges.

Equation 2.4 can now be written as

$$\frac{d\hat{n}_r}{dt} = n(P_{r-1,r}\hat{n}_{r-1} + P_{r+1,r}\hat{n}_{r+1} - P_{r,r-1}\hat{n}_r - P_{r,r+1}\hat{n}_r)$$

$$+ \sum_{s=0}^{K} (P_{s-1,r+1;s,r}\hat{n}_{r+1}\hat{n}_{s-1} - P_{s,r;s-1,r+1}\hat{n}_r\hat{n}_s)$$

$$+ \sum_{s=0}^{K} (P_{s+1,r-1;s,r}\hat{n}_{r-1}\hat{n}_{s+1} - P_{s,r;s+1,r-1}\hat{n}_r\hat{n}_s)$$

$$r = 0,1,2,\ldots,K. \qquad (2.8)$$

Using the condition of detailed balancing, that is,

$$P_{s,r;s-1,r+1} = P_{s-1,r+1;s,r} \exp\left[-\frac{(E_{r+1}-E_r)-(E_s-E_{s-1})}{kT}\right]$$

$$P_{s+1,r-1;s,r} = P_{s,r;s+1,r-1} \exp\left[-\frac{(E_r-E_{r-1})-(E_{s+1}-E_s)}{kT}\right]$$

$$P_{r,r+1} = P_{r+1,r} \exp\left[-\frac{E_{r+1}-E_r}{kT}\right]$$

$$P_{r,r-1} = P_{r,r-1} \exp\left[-\frac{E_r-E_{r-1}}{kT}\right] \qquad (2.9)$$

and dividing Equation 2.8 by $P_{1,0}n^2$, Equation 2.8 becomes

$$\frac{dn_r}{dt'} = \frac{P_{r+1,r}}{P_{10}}\left[n_{r+1} - \exp\left[-\frac{E_{r+1}-E_r}{kT}\right]n_r\right]$$

$$- \frac{P_{r,r-1}}{P_{10}}\left[n_r - \exp\left[-\frac{E_r-E_{r-1}}{kT}\right]\right]$$

$$+ \sum_{s=0}^{K} \frac{P_{s-1,r+1;s,r}}{P_{10}}\left[n_{r+1}n_{s-1} - \exp\left[-\frac{(E_{r+1}-E_r)-(E_s-E_{s-1})}{kT}\right]n_r n_s\right]$$

$$- \sum_{s=0}^{K} \frac{P_{s,r;s+1,r-1}}{P_{10}}\left[n_r n_s - \exp\left[-\frac{(E_r-E_{r-1})-(E_{s+1}-E_s)}{kT}\right]n_{r-1}n_{s+1}\right]$$

$$r = 0,1,2,\ldots,K \qquad (2.10)$$

where $n_r = \hat{n}_r/n$ is the fraction of oscillators in vibrational level r and $t' = nP_{10}t$ is a non-dimensional time. Because the system is closed, the expression

$$\sum_{r=0}^{K} n_r = 1 \qquad (2.11)$$

holds and can be used as a check on the solution.

The above system of nonlinear equations represent the rate equations for the fractional population distribution functions n_r as a function of t'. To obtain solutions of Equations 2.10 expressions are needed for the V-T and V-V

transition probabilities as functions of the translational or heat bath temperature T.

Transition Probabilities

For the V-T energy exchange process given by Equation 2.5, the thermally averaged transition probabilities are based on a one dimensional "head-on" collisional model between two oscillators with an exponential interaction law between the two colliding molecules (30). The V-T collisional transition probabilities used were those of the harmonic oscillator transition probabilities with the energy difference between adjacent levels replaced by the corresponding energy difference $E_{r+1} - E_r$ for the anharmonic oscillator (17). The thermal averaging technique was that described in References 27 and 30 where transition probabilities for individual collisions are averaged over the thermal velocity to arrive at (17, 27)

$$P_{r+1,r} = Z(r+1)\left(\frac{2\pi}{3}\right)^{1/2}\left(\frac{\mu}{kT}\right)^{1/6}\left[\frac{\ell' kT_c}{\hbar}\left[1-\omega_e(2r+1)\right]\right]^{7/3}$$

$$\times \frac{0.08\mu}{h} \exp\left[-\frac{3}{2}\left(\frac{\mu}{kT}\right)^{1/3}\left[\frac{\ell' kT_c}{\hbar}\left[1-\omega_e(2r+1)\right]\right]^{2/3}\right] \quad (2.12)$$

where Z, ℓ' and μ are, respectively, the number of collisions per second experienced by an oscillator with a gas density of one molecule per unit volume, effective range of repulsive forces and reduced mass of the system (in the case of diatomic

oscillators it is equivalent to the mass of the atom). The Boltzmann constant is k, $\hbar$ is $h/2\pi$ and T_c is the characteristic vibrational temperature equal to $h\nu/k$.

The T-V rates given by Equation 2.12 for the higher quantum levels are much higher than the corresponding V-T rates of the Landau-Teller (20) theory. The above equation reduces to the Landau-Teller rate if ω_e is set equal to zero, i.e.,

$$\frac{P_{r+1,r}}{P_{10}} = r + 1 \qquad (2.13)$$

which is no longer temperature dependent.

For the V-V exchange rate probabilities, the calculation was conducted in a fashion described by Fisher and Kummler (11). The molecular model of Rapp and Englander-Golden (34) was used which is a collinear model which results in V-V exchange during "head-on" collisions. Rapp and Englander-Golden (34) used a two-state approximation for the semiclassical calculation of the energy transfer per collision. Basically and briefly, what the preceding statement means is as follows. The semiclassical designation comes from the fact that the trajectory motion between two colliding molecules is treated in a classical mechanics sense while the internal motion of the oscillators is treated with wave mechanics. The two state approximation means that only the initial and final states of the oscillator are treated in the wave equation representing

the oscillator (42). For lower temperatures for which this dissertation is concerned, this two state approximation is a good approximation (11, 42).

The energy transfer probability per collision is given by (11)

$$\hat{P}_{s,r;s+1,r-1} = \sin^2(2\ell'\mu v_o U_{r,r-1} U_{s,s+1}/h)\,\mathrm{sech}^2\left[\frac{\ell' 2E_d}{2\pi v_o}\right] \qquad (2.14)$$

where v_o is the relative velocity when the separation distance between the two colliding is at infinity. The U's are the matrix elements for vibrational transition in the individual molecules and are calculated using harmonic wave functions (42).

In order to convert the transition probabilities of Equation 2.14 to rate constants, they are integrated over the one dimensional Maxwellian velocity distribution (14).

$$\frac{dn}{n} = \frac{\mu}{kT} v_o \exp\left[\frac{-\mu v_o^2}{2kT}\right] dv_o \qquad (2.15)$$

where dn/n is the fraction of incident molecules with velocity between v_o and $v_o + dv_o$. The thermally averaged transition probabilities are then

$$P_{s,r;s+1,r-1} = Z\frac{16\ell^{12}\mu^3 U^2_{r-1,r} U^2_{s,s+1}}{h^2\, kT} \int_o^\infty v_o^3 \exp\left[\frac{-\mu v_o^2}{2kT}\right] \mathrm{sech}^2\left[\frac{\ell' E_d}{\pi v_o}\right] dv_o \qquad (2.16)$$

Equation 2.16 was evaluated by Fisher and Kummler (11) by two approximations depending on E_d. In the present investigation Equation 2.16 was evaluated numerically using Simpson's rule. This was not too time consuming because the integrand is highly peaked about a given value of v_o and for values of v_o very far away from this value the integrand is essentially zero. The reason for evaluating the integral was to obtain values of the V-V rates between the two approximations as used by Fisher and Kummler (11).

Figures 1 and 2 show values of the V-T and V-V transition probabilities obtained from Equations 2.12 and 2.16. Shown are the ratios $P_{r+1,r}/P_{10}$ for the V-T transition probabilities and $P_{s,r;s+1,r-1}/P_{10}$ for the V-V transition probabilities calculated at two heat bath temperatures. In Figure 1, T = 500°K; in Figure 2, T = 1000°K. In both figures, three different V-V transition ratios are plotted for various values of s. Also shown in the figures are V-V and V-T rates as given by formulas from Bray (6) which uses the theory based on Reference 40, these values are shown by the dashed lines. Also shown in Figure 2 are V-T values used in Treanor et al. (46) which are also calculated from the theory of Reference 40. Table 1 presents the V-V transition rates for various values of r when s = 0. It is given mainly as a source for future reference. Values for the V-T rates have been presented elsewhere (27). The values are probabilities per collision.

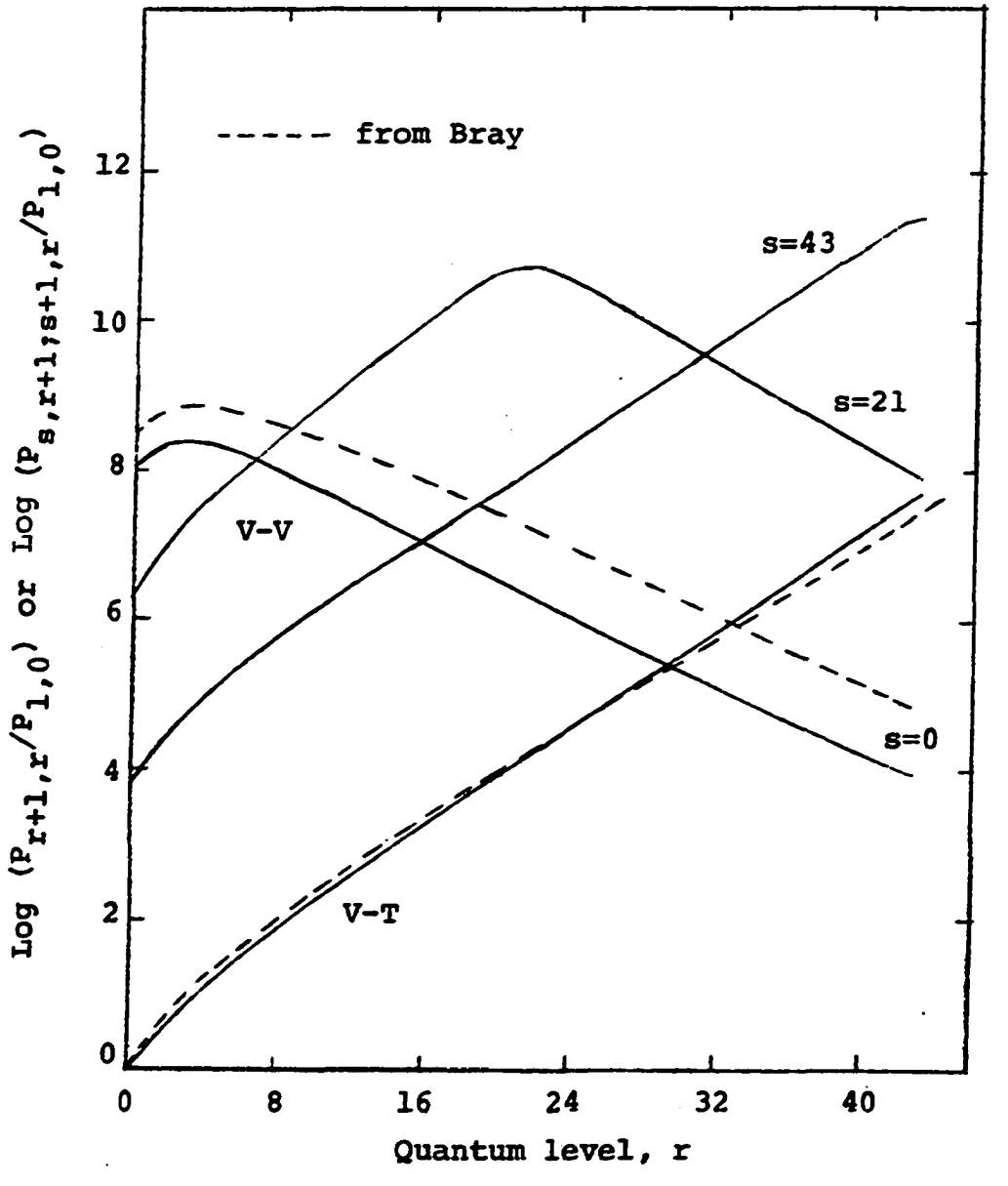

Figure 1. V-V and V-T transition probabilities ratios of T = 500°K
(Ratios from Bray's (6) probabilities also shown.)

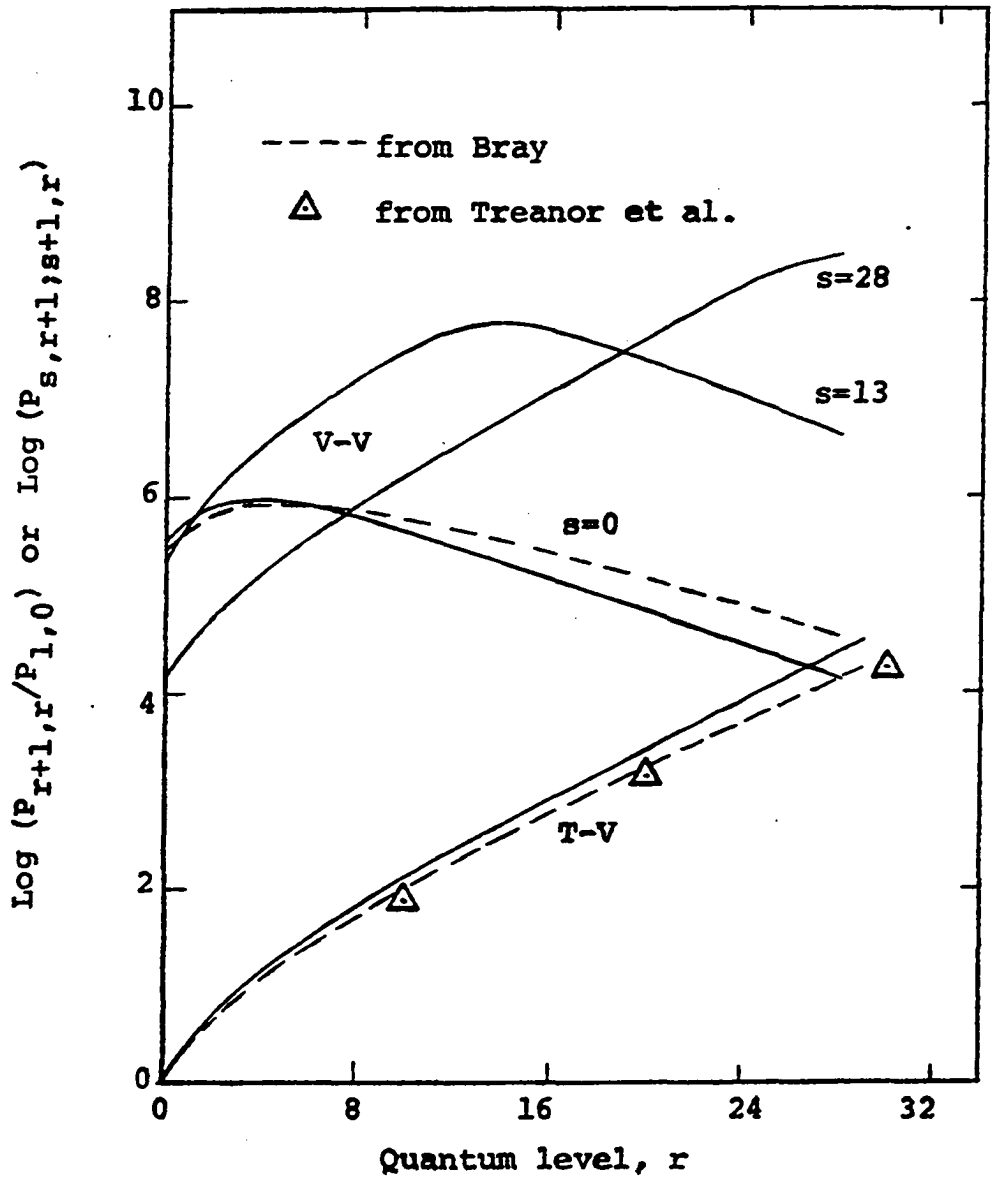

Figure 2. V-V and V-T transition probabilities ratios at T = 1000°K

(Ratios from Bray's (6) probabilities and Treanor et al. (46) also shown.)

Table 1. V-V transition probabilities for T = 500°K and T = 1000°K

r	$P_{0,r+1;1,r}$ (500°K)	$P_{0,r+1;1,r}$ (1000°K)
0	0.1947×10^{-2}	0.3894×10^{-2}
1	0.3511×10^{-2}	0.7373×10^{-2}
2	0.4141×10^{-2}	0.9645×10^{-2}
3	0.4053×10^{-2}	0.1067×10^{-1}
4	0.3590×10^{-2}	0.1072×10^{-1}
5	0.2999×10^{-2}	0.1014×10^{-1}
6	0.2415×10^{-2}	0.9218×10^{-2}
7	0.1900×10^{-2}	0.8146×10^{-2}
8	0.1472×10^{-2}	0.7056×10^{-2}
9	0.1129×10^{-2}	0.6024×10^{-2}
10	0.8605×10^{-3}	0.5088×10^{-2}
11	0.6532×10^{-3}	0.4263×10^{-2}
12	0.4947×10^{-3}	0.3551×10^{-2}
13	0.3742×10^{-3}	0.2945×10^{-2}
14	0.2830×10^{-3}	0.2435×10^{-2}
15	0.2141×10^{-3}	0.2008×10^{-2}
16	0.1621×10^{-3}	0.1653×10^{-2}
17	0.1228×10^{-3}	0.1360×10^{-2}
18	0.9318×10^{-4}	0.1118×10^{-2}
19	0.7080×10^{-4}	0.9182×10^{-3}
20	0.5388×10^{-4}	0.7544×10^{-3}
21	0.4107×10^{-4}	0.6198×10^{-3}
22	0.3136×10^{-4}	0.5094×10^{-3}
23	0.2398×10^{-4}	0.4188×10^{-3}
24	0.1837×10^{-4}	0.3445×10^{-3}
25	0.1409×10^{-4}	0.2835×10^{-3}
26	0.1083×10^{-4}	0.2335×10^{-3}
27	0.8340×10^{-5}	0.1924×10^{-3}
28	0.6431×10^{-5}	0.1587×10^{-3}

Table 1. (Continued)

r	$P_{0,r+1;1,r}$ (500°K)	$P_{0,r+1;1,r}$ (1000°K)
29	0.4967×10^{-5}	
30	0.3843×10^{-5}	
31	0.2977×10^{-5}	
32	0.2310×10^{-5}	
33	0.1795×10^{-5}	
34	0.1397×10^{-5}	
35	0.1089×10^{-5}	
36	0.8501×10^{-6}	
37	0.6644×10^{-6}	
38	0.5200×10^{-6}	
39	0.4076×10^{-6}	
40	0.3198×10^{-6}	
41	0.2513×10^{-6}	
42	0.1977×10^{-6}	
43	0.1557×10^{-6}	

It should be mentioned that the reason for the difference between Bray's V-V values and the values obtained from Equation 2.16 is due to the fact that the corresponding P_{10} differ by an order of magnitude and not the V-V rates. From these figures, it is easy to see why Treanor et al. (46) called their analysis V-V dominated when they used only the lower quantum levels in their reported research. Finally, the values of P_{10} for the two temperatures are: $P_{10} = 0.1644 \times 10^{-10}$ for $T = 500°K$ and $P_{10} = 0.1242 \times 10^{-7}$ for $T = 1000°K$.

Anharmonic Vibrational Relaxation of Treanor et al.

As previously mentioned in Chapter I, Treanor et al. (46) used a Chapman-Enskog expansion procedure to order the terms in the master relaxation equation in order to calculate the secular change of the distribution due to the V-T exchanges. The basis for this (refer to Figures 1 and 2) is that for the lower quantum levels the V-V rates are much, much greater than the V-T rates; therefore, in a very short time scale called $\tau_{VV} = O[(P_{0,1;1,0})^{-1}]$ (46) there will be an initial adjustment into a quasisteady distribution. The secular change of the quasisteady distribution which occurs in a time scale $\tau_{VT} = O[(P_{10})^{-1}]$ is calculated according to the above mentioned Chapman-Enskog procedure. Again, the above procedure is presumably valid for the case when V-V rates are much larger than V-T rates (for their work (46) they set K = 25 as an upper limit.)

To arrive at their zeroth order and first order equations proceed as follows. Introduce the ordering parameter

$$\varepsilon = P_{10}/P_{0,1;1,0} \tag{2.17}$$

and define

$$P'_{sr} = P_{sr}/\varepsilon$$

so that V-T and V-V exchange probabilities are of the same order. Expand the time derivative and distribution function

in powers of ε, i.e.,

$$\frac{d}{dt'} = \varepsilon \frac{d}{dt}\Big|_0 + \varepsilon^2 \frac{d}{dt}\Big|_1 + \ldots$$

$$n_r = n_r^{(0)} (1 + \varepsilon \phi_r^{(1)} + \varepsilon^2 \phi_r^{(2)} + \ldots), \qquad (2.18)$$

where d/dt' and Φ's are the order of one. Substitute Equation 2.18 into Equation 2.10. The superscripts 0, 1, etc. refer to the zeroth order, first order, etc. By grouping according to powers of ε and setting coefficients of like powers to zero results in the following two equations:

For ε^0:

$$\sum_{s=0}^{K} P_{s-1,r+1;s,r}\left[n_{r+1}^{(0)} n_{s-1}^{(0)} - \exp\left[-\frac{(E_{r+1}+E_{s-1}-E_r-E_s)}{kT}\right] n_r^{(0)} n_s^{(0)}\right]$$

$$\sum_{s=0}^{K} P_{s,r;s+1,r-1}\left[n_s^{(0)} n_r^{(0)} - \exp\left[-\frac{(E_r+E_s-E_{s+1}-E_{r+1})}{kT}\right] n_{s+1}^{(0)} n_{r-1}^{(0)}\right] = 0$$

(2.19)

and for ε':

$$\frac{dn_r^{(0)}}{dt'}\Big|_0 - \frac{P'_{r+1,r}}{P_{1,0}}\left[n_r^{(0)} - \exp - \frac{E_{r+1}-E_r}{kT} n_r^{(0)}\right]$$

$$- \frac{P'_{r,r-1}}{P_{1,0}}\left[n_r^{(0)} - \exp - \frac{E_r - E_{r-1}}{kT} n_{r-1}^{(0)}\right]$$

$$= \sum_{s=0}^{K} \frac{P_{s-1,r+1;s,r}}{P_{1,0}} \left[n_{r+1}^{(0)} n_{s-1}^{(0)} \left(\phi_{r+1}^{(1)} + \phi_{s-1}^{(1)} \right) - \exp\left[-\frac{(E_{r+1}+E_{s-1}-E_r-E_s)}{kT} \right] \right.$$

$$\left. n_r^{(0)} n_s^{(0)} \left(\phi_r^{(1)} + \phi_s^{(1)} \right) \right] - \sum_{s=0}^{K} \frac{P_{r,n;s+1,r-1}}{P_{1,0}} \left[n_r^{(0)} n_s^{(0)} \left(\phi_r^{(1)} + \phi_s^{(1)} \right) \right.$$

$$\left. - \exp\left[-\frac{(E_r+E_s-E_{s+1}-E_{r-1})}{kT} \right] n_{r-1}^{(0)} n_{s+1}^{(0)} \left(\phi_{s+1}^{(1)} + \phi_{r-1}^{(1)} \right) \right] \qquad (2.20)$$

Solution of the nonlinear Equation 2.19 results in the quasi-steady distribution or the frequently mentioned Treanor distribution

$$n_r^{(0)} = n_0^{(0)} \exp(-r\gamma) \exp(-E_r/kT) \qquad (2.21a)$$

where γ is a parameter for all levels and is equal to zero for a Boltzmann distribution. They then redefine γ in terms of a parameter θ_1^*, which can be thought of as a "vibrational temperature" of the first quantum level, such that Equation 2.21a becomes

$$n_r^{(0)} = n_0^{(0)} \exp(-rE_1/k\theta_1^* + [(rE_1-E_r)/kT]) \qquad (2.21b)$$

For the isothermal heat bath case $n_0^{(0)}$ and θ_1^* will vary as functions of time. If θ_1^* is much, much greater than T a population inversion of the quasisteady distribution will occur. The zeroth order or quasisteady distribution, given by Equation 2.21b, variation with respect to time can be

calculated using the first moment equation of the master relaxation equations (the first moment of the first order equation would have the same result (15)) with the zeroth order solution substituted into the master equations. The first moment result is (46)

$$\frac{d\bar{V}}{dt'} = n_0^{(0)} (\exp[E_1/k\theta_1^* - E_1/kT]-1) \times \sum_{r=0}^{K} \frac{P_{r+1,r}}{P_{1,0}} \left[\frac{n_{r+1}^{(0)}}{n_r^{(0)}}\right] \tag{2.22}$$

where

$$\bar{V} = \sum_{r=0}^{K} r\, n_r^{(0)} \tag{2.23}$$

and $\bar{V}$ is called the average number of vibrational quanta. With initial conditions given the time variation of the zeroth order solution can be calculated using Equations 2.21a, 2.22 and 2.23. Note that for harmonic oscillators and Landau-Teller transition probabilities Equation 2.22 will reduce to the Bethe-Teller equation (27). They conclude that acceleration of de-excitation rates over corresponding excitation rates is a result of the population inversion witnessed in the zeroth order solution. This inversion causes an increase in the de-excitation rate because at higher quantum levels V-T rates are larger than at lower levels and the removal of quanta will be hastened by the fact that there are more vibrational quanta in

the upper levels than would be for a Boltzmann distribution (Landau-Teller type relaxation). Because the Treanor et al. (46) solution is dependent upon the premise that V-V probability rates are significantly larger than the V-T probability this truncated model may be in error under certain conditions as discussed previously in Chapter I. Bray's (6) full solution substantiates this. No information is available in Treanor's solution as to how the population distribution behaves prior to the quasisteady state and to what effect this can have on values at the quasisteady state. Furthermore, time variation of the Treanor distribution is accomplished only through a first moment method (Equation 2.22). Before discussing Bray's (6) solution to the expansion flow problem, it would be of interest to discuss the significance of Equation 2.20.

In reviewing Equation 2.20, it can be seen that if the zeroth order solution is known, then the first order correction to the zeroth order distribution should in theory be given by the solution to Equation 2.20. Difficulties with the author's attempt to solve this equation and further discussion of this first order solution will be delayed until Chapter III. This first order correction should allow for a more exact solution to the vibrational population distribution function.

Bray's Full Solution

Because the basic equations for the theoretical calculation of the vibrational distribution function n_r have been presented, a more informative description of Bray's solution (6) to the expansion flow problem will now be given. Bray's full solution for the isothermal heat bath involved the solving of the master relaxation equations (Equation 2.10), an assumed distribution form for the vibrational population distribution and a first moment equation of the master relaxation equations given by

$$\frac{d\bar{V}}{P_{10}ndt} = - \sum_{r=0}^{K} (P_{r,r-1}n_r - P_{r-1,r}n_{r-1}) \qquad (2.24)$$

The solution starts by assuming an initial distribution equivalent to Equation 2.21b, which is repeated here with the superscripts removed,

$$n_r = n_0 \exp\left[- \frac{rE_1}{k\theta_1^*} + \left[\frac{(rE_1 - E_r)}{kT}\right]\right] \qquad (2.21b)$$

where θ_1^* corresponds to Y of Bray's notation. Again, because of the assumed initial form (Equation 2.21a), his solution begins at some time other than initial nonequilibrium, and in fact, the time corresponds to the V.V. equilibrium or quasi-steady state time of the Treanor et al. (46) solution.

His solution is an iterative technique involving Equations 2.10, 2.24 and 2.21a whereby the initial Treanor distribution is corrected to the "full solution" at some given value of θ_1^*. (Bray's iterative technique involves more complication than the above three equations i.e., they are put into a form more amenable to iterative technique, for a thorough discussion of his iterative technique see Reference 5.)

Basically, his solution allows for the upper levels of the vibrational distribution to be corrected according to the V-T terms in Equation 2.10 for large quantum values, because at these values V-T exchange rates exceed V-V exchange rates. To repeat from Chapter I, he shows that the upper level populations are Boltzmann while the lower levels follow the Treanor distribution. Furthermore, Bray does not have to allow for truncation of the anharmonic model.

Bray (6) also studies the relaxation rate of θ_1^* versus that for θ_1^* relaxation rate of Landau-Teller by using the following definition:

$$\psi = \frac{d\theta_1^*/dt}{d\theta_1^*/dt)_{L.T.}} \tag{2.25}$$

where $)_{L.T.}$ refers to Landau-Teller. In Figure 3 is a graph taken from Bray's reported work (6) showing typical vibrational population distributions for nitrogen with $\theta_1^* = 3000°K$ and

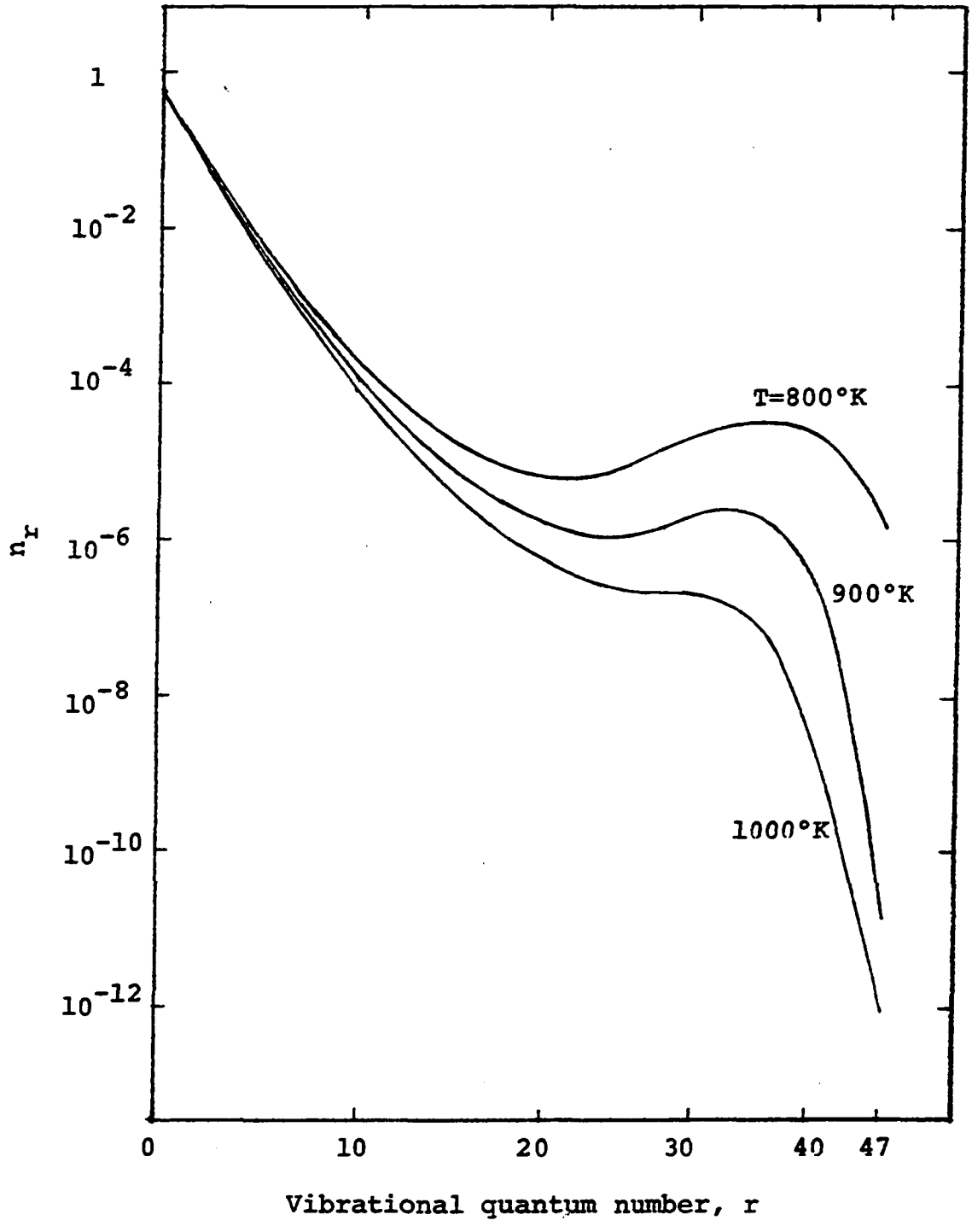

Figure 3. Vibrational population distribution for Bray's (6) full solution when $\theta_1^* = 3000°K$ and three different values of T

three different values of T. He concludes that a large increase in ψ is associated with the appearance of the peak in Figure 3 as T decreased (i.e. increasing inversion). Further, large increases in ψ occur only when θ_1^*/T is greater than 3. Again, all reported calculations are for one point in time, i.e., at a time from initially nonequilibrium such that an initial Treanor distribution can exist. From the method of solution, the Bray solution could properly be termed a moment method as is the Treanor et al. (46) solution.

Although Hsu and Maillie (16, 17) do calculate the time variation of population distributions from a given initial conditions in their V-T dominated model, they ignore the transient period between initial nonequilibrium and the quasi-steady state. Their V-T solution is the integration of Equation 2.10 with the V-V terms set to zero and using an initial Treanor distribution. The basic objective of the present work can now be better understood than was stated in Chapter I in light of the previous discussion. The time integration of the complete master relaxation equations for the physical model considered will be done without any modification of that model, i.e. no ignoring of transient effects and no a priori distribution will be assumed. From these solutions relaxation rates will be calculated.

Numerical Techniques

The master relaxation equations, given by Equation 2.10, represent a system of nonlinear ordinary differential equations with the nondimensional time t' taken as the independent variable. For purposes of discussion in this section, the equations will be written in matrix notation in the following form

$$\frac{d\underline{n}}{dt'} = \underline{F}\ (\underline{n}) \tag{2.26}$$

where $\underline{n}$ represents the vector whose elements are $n_o, n_1, \ldots n_K$, and $\underline{F}$ is the vector whose elements are functions of the vector $\underline{n}$ and represents the right hand side of Equation 2.10. When initial conditions for $\underline{n}$ are specified Equation 2.26 is properly posed for integration.

The master relaxation equations belong to a class of ordinary differential equations that present no conceptual difficulties for numerical integration by explicit methods, such as Runge-Kutta and various predictor-correctors algorithms. In fact, these methods will do the numerical integration, but, unfortunately, stability criteria of these explicit methods severely limits the maximum stepsize allowable. And, if any reasonable range of the independent variable needs to be calculated, computing time soon becomes enormously large. The numerical difficulties of Equations 2.26 is due to the fact

that the eigenvalues of the matrix $\underline{F}$, if the equations are linear, or the Jacobian of $\underline{F}$, if equations are nonlinear, differ in magnitude by a large amount (of course, for nonlinear equations the magnitude of the eigenvalues will change as time proceeds). Such a system of equations are termed "stiff" (40) because of the "parasitic" eigenvalues. It is these "parasitic" eigenvalues that cause the sophisticated explicit methods, such as Runge-Kutta, predictor-corrector, etc. to demand small stepsizes for stability reasons. Problems involving stiff equations also arise in the area of chemical nonequilibrium (22-25, 26, 41, 47).

Lomax and associates (22-25) separate the eigenvalues of the stiff system into two groups or classes, parasitic and driving eigenvalues. If the magnitude of the driving eigenvalues were scaled so that they were the order of one, then the value of the parasitic would be much, much greater than one. It is the values of these driving eigenvalues that result in what is seen on a graph paper when the values of $\underline{n}$ are plotted for any reasonable length of time.

Before continuing the discussion of the numerical method that allows the solution of the above type of system, it should be pointed out that at very small times, where the effects of the parasitic eigenvalues are important, an explicit method was used and its characteristics were most desirable. A predictor-corrector algorithm developed by Crane

(10) called NODE was obtained from the Iowa State University Computation Center and used throughout the initial stages of nonequilibrium. The reason for this was because the effects of the initial nonequilibrium phase wanted to be studied. This requires a small stepsize and the use of the implicit method developed for the "stiff" problem would require too much time at these small stepsizes required for the initial integration. Furthermore, a feature of the NODE program that is very practical is its ability to decrease or increase stepsize as accuracy criteria dictate. It was through this feature that led to the use of the implicit method that was used for a large share of the numerical calculations. Basically, what happens to the system of equations (Equation 2.26) is that as the derivative values become smaller, the rate of change of these derivatives also becomes small. At this time accuracy criteria will dictate an increase in stepsize, but as stated earlier stability demands that stepsize remain small. Even though eigenvalues are not explicitly calculated by this technique, or most numerical techniques for that matter, their values actually are related to the stability and accuracy of the solution (22, 25). That is, numerical methods actually act as if the eigenvalues had been calculated.

Implicit methods are generally far superior to explicit methods in terms of stability and the only limitation comes in terms of accuracy and machine time (40) per step. Machine

time usually goes up because of the inversion of a matrix, calculation of Jacobian matrix, or iteration to a solution. The implicit method to be described was used here because it allowed for the large increase in stepsize over explicit methods but still kept truncation error within reasonable bounds.

The method chosen for the present problem is an implicit method that results in the solving of a set of linear algebraic equations. The steps to arrive at the final numerical algorithm was patterned after that given in Reference 44. As is shown in the Appendix the final step by step solution is equivalent to another method suggested by Lomax and Bailey (25) for "stiff" systems but with one minor time saving difference. To continue with the development of the method, on the right hand side of Equation 2.26 replace each $n_o, n_1, \ldots, n_K$ by

$$\frac{n_{r,i} + n_{r,i+1}}{2} \tag{2.27}$$

where the subscript i refers to reference step location. Because of the nonlinearity of the master relaxation equations, terms of the form $n_r n_s$ appear. These terms are replaced according to the following formula (29)

$$n_{r,i+1} n_{s,i+1} = -n_{r,i} n_{s,i} + n_{r,i} n_{s,i+1} + n_{r,i+1} n_{s,i} \tag{2.28}$$

Equation 2.24 becomes after algebraic manipulation equivalent to the following vector equation

$$\frac{d\underline{n}}{dt'} = \frac{1}{2} [A_i] \underline{n}_{i+1} + \frac{1}{2} \underline{f}_i \tag{2.29}$$

where $[A_i]$ is the Jacobian matrix of $\underline{F}$ at the point $t' = iH$ where H is the stepsize; elements of $[A_r]$ are

$$a_{\ell j} = \frac{\partial F_\ell}{\partial n_j} \tag{2.30}$$

The indices ℓ and j denote the ℓth and jth elements in the $\underline{F}$ and $\underline{n}$ vectors, respectively. $\underline{f}_i$ is a column vector that contains only the linear terms of the original vector F at the step $i = t'/H$. The left hand side of Equation 2.26 is replaced by

$$\frac{\underline{n}_{i+1} - \underline{n}_i}{H} \tag{2.31}$$

so that the final operating equation becomes the solving of the following set of linear algebraic equations

$$[I - \tfrac{1}{2}H A_i] \underline{n}_{i+1} = \underline{n}_i + \tfrac{1}{2}H \underline{f}_i \tag{2.32}$$

where I is the identity matrix. Solution of Equation 2.32 was based on a Gaussian reduction technique. This method is documented under the title UGELG and is available from the Iowa State Computation Center.

As is shown in the Appendix the present method is equivalent to the method studied by Lomax and associates (22-25) where they first linearized Equation 2.26 using a Taylor series expansion about the ith reference step and then applied the modified implicit Euler method to these linearized equations to arrive at

$$(I - \tfrac{1}{2}H\,A_i)\underline{n}_{i+1} = (I - \tfrac{1}{2}H\,A_i)\underline{n}_i + H\underline{F}_i + O(H^3) \qquad (2.33)$$

It is Equation 2.33 that is studied quite thoroughly in the Lomax papers (22-25) and its use is highly recommended for systems of equations with many large parasitic eigenvalues present. Since local linearization of the derivative has an error the order of H^2, the implicit Euler method which has an error the $O(H^3)$ is consistent and using any more exact methods is not warranted (25). The main advantage of using Equation 2.32 instead of Equation 2.33 is computing time. In experimental runs to check the truncation error of Equation 2.32, the method given by Equation 2.32 was found to be approximately 30% faster than the method given by Equation 2.33. Also, the truncation error between the two methods was consistent with the error bound.

Stability and accuracy were studied and evaluated according to the following statement that summarizes the discussion and numerical experiments performed by Lomax and his associates (22-25) when dealing with stiff equations.

Briefly, then, for equations which involve parasitic eigenvalues and driving eigenvalues, they (22-25) state that in order to provide accurate and usable solutions to stiff systems the method should be stable for the large negative real values of the eigenvalues and accurate and stable for the much smaller eigenvalues. What this says then is choose the stepsize to resolve the effects of the driving eigenvalues without any regard to the parasitic eigenvalues as long as the method is stable for the parasitic eigenvalues. In theory, then, this implies that an increase in stepsize corresponding to the difference in magnitude between the two classes of eigenvalues should be realized if a method such as that given by Equation 2.32 or 2.33 is used instead of an explicit method because stability exists for all real negative eigenvalues (24). Although the numerical method did not require the calculation of local eigenvalues, periodic calculations were nevertheless made to determine an order of magnitude for the stepsize and to check the sign on the eigenvalues. Continued discussion of the numerical techniques used will be delayed until Chapter III.

CHAPTER III. RESULTS AND DISCUSSION

Introductory Remarks

In this chapter the significant results of the numerical integration of the master relaxation equations will be presented and discussed. Diatomic nitrogen was used as the model gas for all calculations and molecular constants for nitrogen are (8, 27):

$$\mu = 4.6872 \times 10^{-23} \text{ grams}$$

$$\nu = 0.7082 \times 10^{14} \text{ cycles/sec}$$

$$\ell' = 1.25 \text{ angstroms}$$

$$k = 1.3805 \times 10^{-16} \text{ erg/°K}$$

$$\hbar = 1.0545 \times 10^{-27} \text{ erg-sec}$$

$$d_e = 1.56 \times 10^{-11} \text{ ergs}$$

The initial equilibrium distribution was a Boltzmann distribution at a temperature T_V

$$n_r = \frac{\exp(-E_r/kT_V)}{\sum_{r=0}^{K} \exp(-E_r/kT_V)} \tag{3.1}$$

Two different temperature combinations are reported in this chapter. One temperature combination was $T_V = 4000°K$ initially and $T = 1000°K$ (T is the heat bath temperature). For this case three different total number of vibrational levels were

calculated, i.e., 30, 18 and 11 level models were investigated. The other temperature combination was T_V = 2500°K initially and T = 500°K. For this case, a 45 level model and 11 level model were chosen to be investigated. The ratio of T_V/T is greater than or equal to 4 for both temperature cases to correspond to conditions set forth in Reference 46 where it was concluded that for diatomic nitrogen any enhancement of the de-excitation rate must necessitate a ratio of the above or larger (45).

There were two primary reasons for choosing different values for the total number of vibrational levels. First the lower level models, i.e., 11 and 18 were chosen to check the numerical procedure and to use as a comparison for the larger level models. Secondly, the larger level models should show the effects of both the V-V dominated lower levels and the V-T dominated upper levels. Reference to Figures 1 and 2 show that this will be true for the 45 level model, and V-T effects should appear in the 30 level model but not to the same extent as the 45 level model. However, one of the major handicaps of these larger level models is the excessive computer time required, even for the calculations when the implicit numerical method was used. The main reason for this is a result of the summation terms on the right hand side of the master relaxation equations, i.e., Equations 2.10. Also, as will be discussed at the conclusion of this chapter, accuracy

considerations for the implicit method required smaller stepsizes as K was given the largest values for each of the temperature cases. Therefore, computation was stopped for the large K cases when the region of high de-excitation rates was traversed. In the terminology of Treanor et al. (46), this early stage of relaxation may loosely be called the τ_{VV} time regime.

All numerical computations were done using the IBM 360-65 computer of the Iowa State Computation Center. It should be stated again that the programs for solving the set of algebraic equations in the implicit technique, for explicit integration and for calculating eigenvalues were obtained from the Iowa State Computation Center Library. As an aid to the following discussion, the results presented for T_V = 2500°K and T = 500°K will sometimes be referred to as the low temperature case while the results for T_V = 4000°K and T = 1000°K will occasionally be referred to as the high temperature case.

In all the following figures where a time appears it will be the nondimensional time $t' = P_{10}nt$. This quantity can also be interpreted as the average number of quanta transferred between level 1 and level 0 in time interval t (17). For the low temperature case a nondimensional time at one atmosphere pressure is approximately 1/10 of the dimensional time and for the high temperature case a nondimensional time is approximately 20 times larger than dimensional time. Also, results will not

be presented nor were they calculated for times corresponding to complete equilibrium because the goal of this research was to investigate relaxation behavior in the early stages of vibrational nonequilibrium. That is, the effects of anharmonicity should have the most effect in this early time regime.

Vibrational Population Distributions

In this section graphs will be presented that show the level population densities n_r vs quantum number r with the nondimensional time taken as the parameter for the curves. It will be noted that the abscissa scale representing the quantum number r is not a linear relationship scale, but is calculated so that a Boltzmann distribution will appear as a straight line. Presentation of the vibrational population distributions give better comparison between the various individual population densities than a group of curves showing the individual population density versus time. Also, it should be noted that vibrational population distribution curves occurring between the times given parametrically will lie somewhere between the curves corresponding to the two times unless otherwise noted.

Figures 4-6 taken collectively represent the changes in the vibrational population distribution from $t' = 0.0$ to 6.27×10^{-2} for $T_V = 2500°K$, $T = 500°K$ and 45 levels. Figure 4 shows the initial readjustment of population densities with

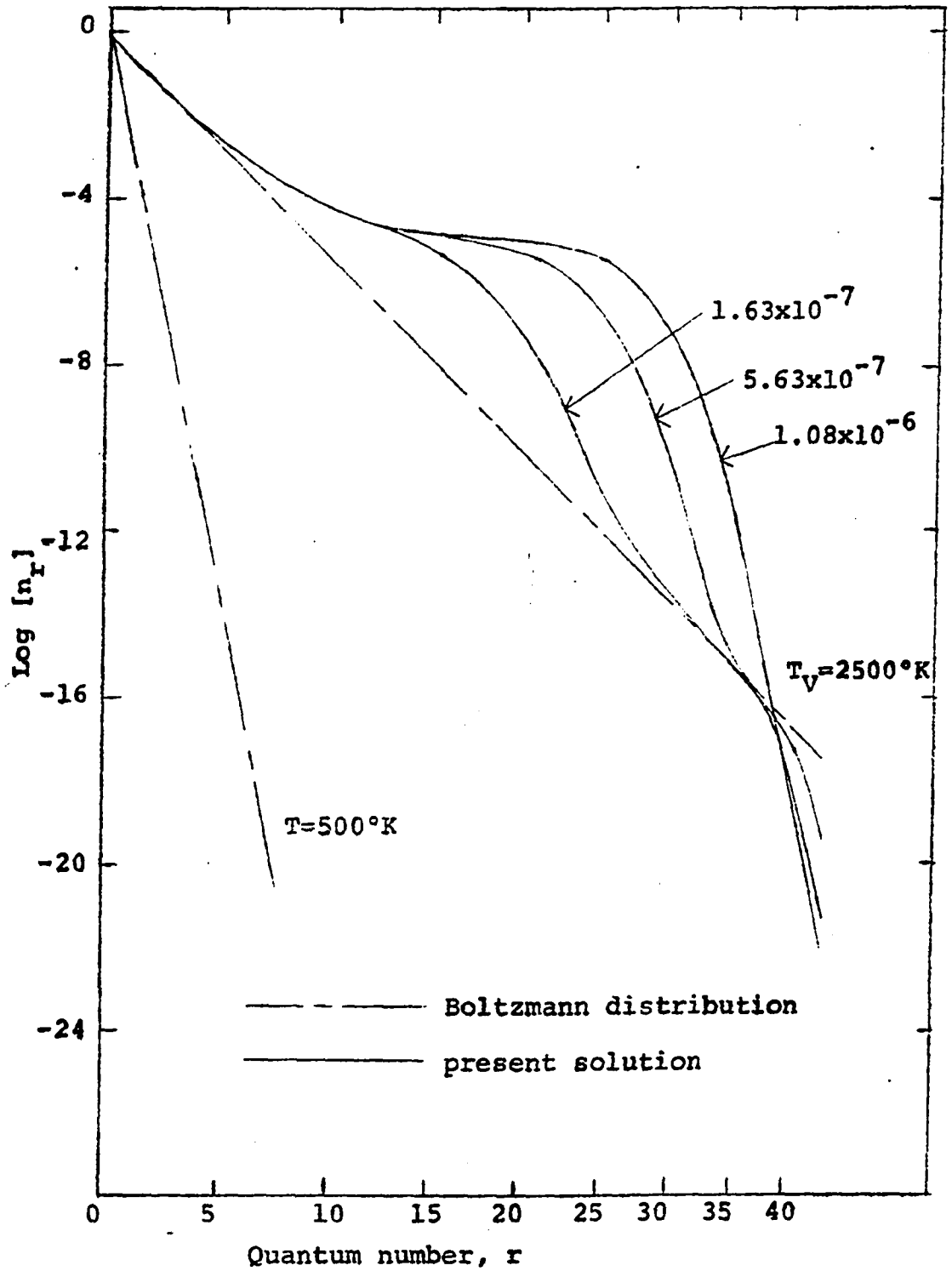

Figure 4. Population distribution for T_V=2500°K, T=500°K and K=44 with $t'=nP_{10}t$ as the parameter

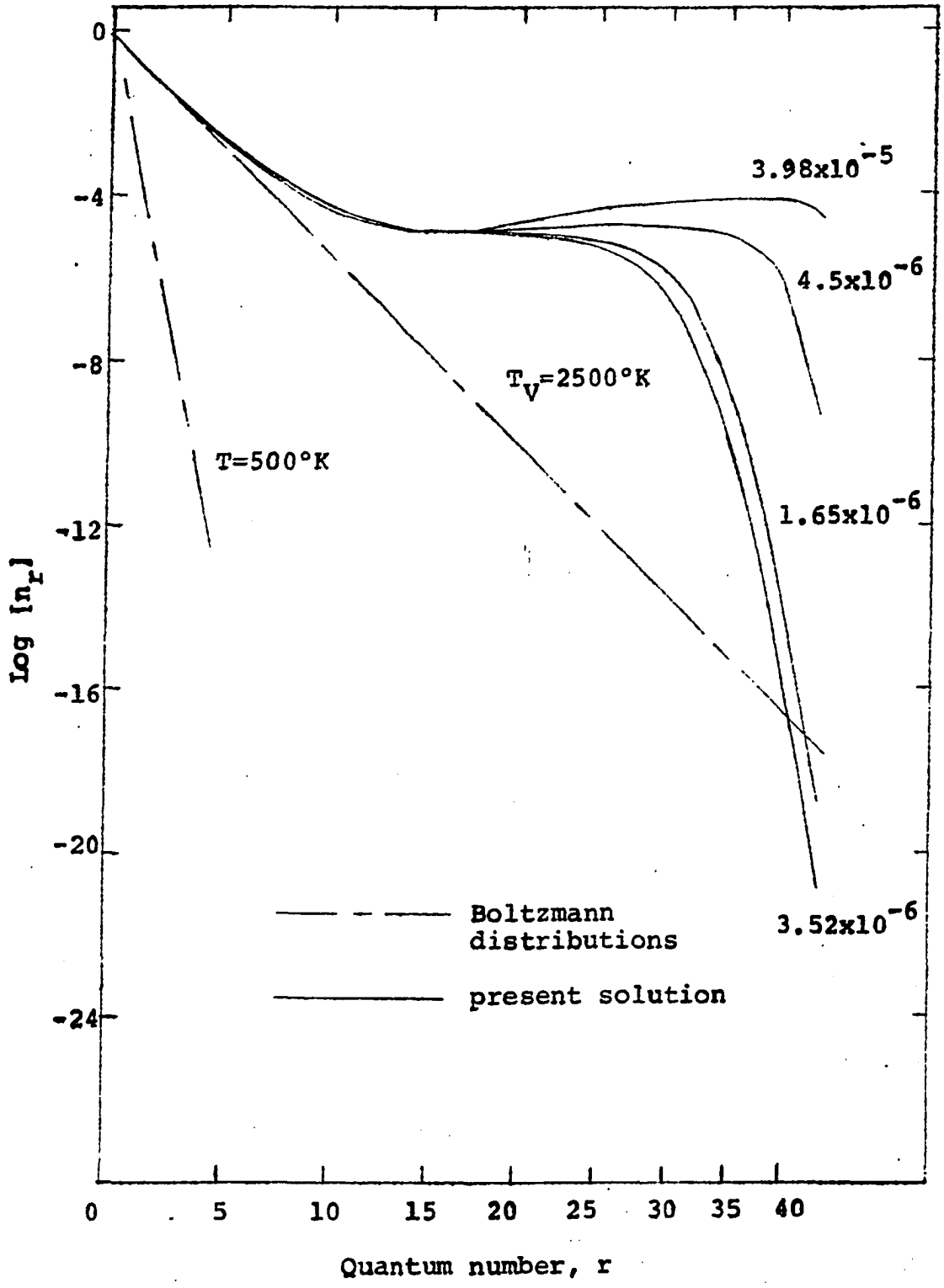

Figure 5. Population distribution for T_V=2500°K, T=500°K and K=44 with t'=P_{10}nt as the parameter

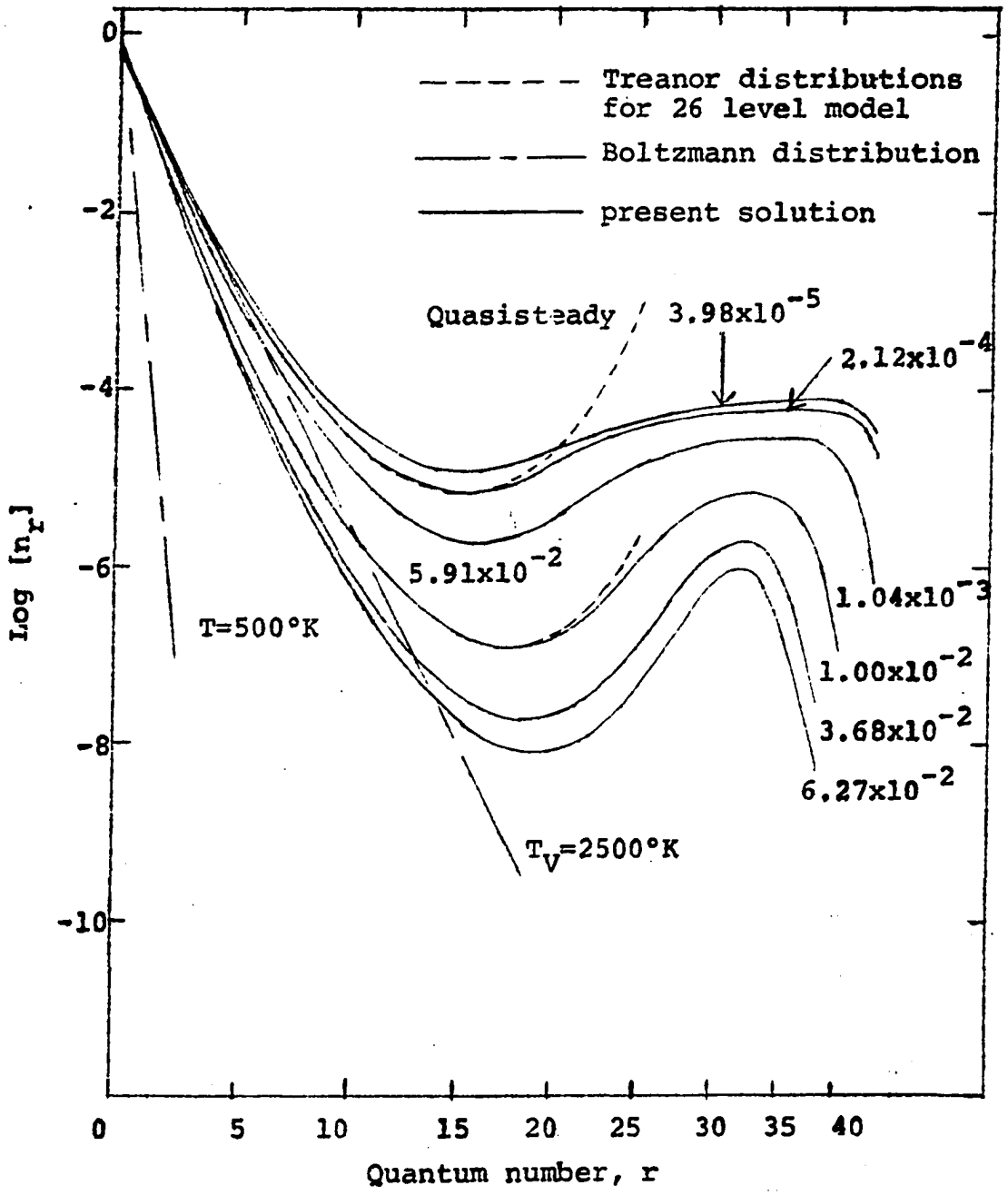

Figure 6. Population distribution for T_V=2500°K, T=500°K and K=44 with $t'=nP_{10}t$ as a parameter. Also shown are Treanor distribution at quasisteady state and later time

very little change in vibrational energy. The initial Boltzmann distribution changes to a highly non-Boltzmann distribution at $t' = 1.08 \times 10^{-6}$. It can be seen that during this time the intermediate levels (say, 12 to 22) form a plateau while the upper levels (34 to 44) approach a Boltzmann distribution corresponding to a temperature of 500°K as indicated by the line labeled 500°K on this graph. At the time $t' = 1.08 \times 10^{-6}$ the uppermost level ($r = 44$) reaches a minimum value for the times considered in the total three graphs.

The curves in Figure 5 show how the population distribution changes up to a time equal to 3.98×10^{-5}. Associated with this curve the dimensionless energy

$$\bar{E}_V = \frac{1}{h\nu} \sum_{r=0}^{K} rE_r \tag{3.2}$$

reaches a maximum value.

Figure 6 is a graph of various population distributions from nondimensional time 3.98×10^{-5} (also shown in Figure 5) to 6.27×10^{-2}. Note that the ordinate scale is expanded in this figure. Also shown on this figure are curves of a Treanor V-V quasisteady distribution for a 26 level model and another curve at $t' = 5.91 \times 10^{-2}$ using the Treanor first moment time variation (17). This latter time is calculated on the basis that V-V quasisteady equilibrium for the Treanor model occurs at $t' = 2.12 \times 10^{-4}$. This latter curve shows

that as time progresses the lower levels maintain a Treanor distribution, but the particular time variation occurs at a faster rate for the complete model as will be shown in the discussion of the relaxation rates.

It will be remembered that the initial Treanor distribution is calculated on the basis that the average number of vibrational quanta, defined by

$$\bar{V} = \sum_{r=0}^{K} r n_r \tag{3.3}$$

is a constant from initial nonequilibrium to the V-V quasi-equilibrium state. The distribution corresponding to $t' = 2.12 \times 10^{-4}$ has an average number of vibrational quanta equal to that at time zero. Comparison between this distribution and the Treanor V-V equilibrium distribution shows high correlation for the lower 18 levels. Referring to Figure 1 shows that for these levels the V-V probabilities are at least 10^3 greater than the V-T exchange probabilities; consequently, good agreement is not surprising, but it is to be expected when the Treanor model is valid. To amplify this statement, if a Treanor V-V equilibrium distribution were calculated using 40 vibrational levels then there would be very little agreement between this distribution and that distribution corresponding to $t' = 2.12 \times 10^{-4}$. It is possible to say that Treanor V-V equilibrium occurs at $t' = 2.12 \times 10^{-4}$ for this case.

Bray (6) also assumes a certain time has elapsed so that a θ_1^* can be defined, hence, a Treanor distribution for lower levels. Bray then iterates on this to arrive at his full solutions. The interesting conclusion to be drawn in studying the various plots of Figure 6 is the form of the distribution is similar to those of Figure 3 which are Bray's full solution near a quasisteady state for various conditions of a defined θ_1^* and T. Although Bray (6) does not present any time variations of his full solution, it is certainly possible to do so (see Reference 5 for details) by using the time variation of the first moment equation. At times corresponding to V-V equilibrium in the sense used by Treanor et al. (46) and Bray (6) the solution to the master relaxation equations substantiate what the above two authors (6, 46) stated, i.e., that the lower levels follow a Treanor distribution while the intermediate levels are a transition between lower V-V dominated lower levels and the V-T dominated upper levels which at times around 2.12×10^{-4} include very few levels. It can only be hypothesized that if the complete anharmonic model ($\tilde{=}$ 53 levels) were used the upper levels would follow a distribution similar to that given by Boltzmann distribution at a temperature of 500°K.

As time increases from $t' = 2.14 \times 10^{-4}$ the inversion plateau gives way to a more peaked distribution and the upper levels become more Boltzmann in appearance (reference to t' =

1.04×10^{-3} distribution). The lower three time curves have only the first 41, 39 and 39 levels plotted, respectively. This is because as the upper levels approach values in the 10^{-8} to 10^{-7} range oscillations (damped, by the way) begin to appear that physically have no justification and furthermore are suspected to be accuracy problems as will be explained later. It is emphasized here, that these oscillations are dependent on the stepsize used in the implicit method at these particular times. For financial reasons, the stepsize was not decreased to correct the accuracy problems, rather the stepsize was kept constant ($\tilde{=} 10^{-4}$) and these upper levels were dropped to yield equations involving lower number of levels. As a result of check cases run using 41 or 39 level models in the region where the upper 5 levels are small in magnitude below approximately 10^{-7}) the lower level results agree to the accuracy desired. Furthermore, whenever the value of the upper levels goes below the 10^{-7} limit its effect upon lower levels is minimal. Again, more discussion of accuracy will be presented later.

Figure 7 is a graph showing vibrational population distributions for T_V = 2500°K, T = 500°K and K = 10. Distributions for various times between 0.0 and t' = 1.0 are shown. The distribution at 5.77×10^{-3} is that distribution for which $\bar{V}$ is equal to the initial $\bar{V}$. Also shown are two distributions using the Treanor et al. (46) method for 11 level system. At

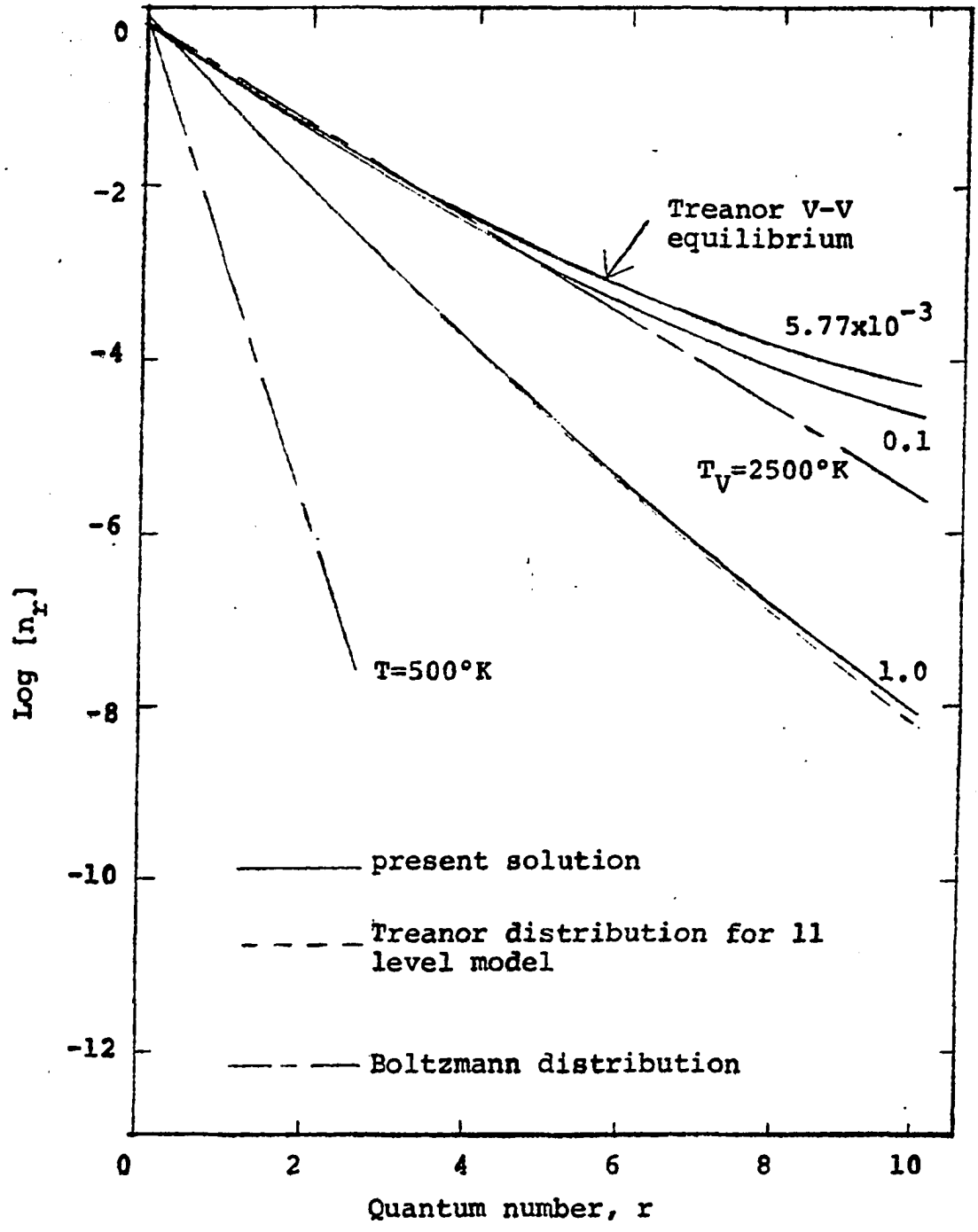

Figure 7. Population distribution for T_V=2500°K, T=500°K and K=10 with $t'=nP_{10}t$ as the parameter. Also shown is a Treanor distribution for an 11 level model

initial V-V equilibrium the distribution is not distinct from that of the $t' = 5.77 \times 10^{-3}$ population distribution. However, at $t' = 1.0$ there is some difference but not to a great extent. Therefore for this low level model, the integration of the full equations agrees quite accurately with the Treanor theory. (The difference between $t' = 1.0$ in the Treanor method and the present method is 5.77×10^{-3}.) Also, the distribution corresponding to maximum vibrational energy is very close to the 5.77×10^{-3} distribution and for that reason was not plotted.

In Figures 8-11 vibrational population distributions are shown for the cases where $T_{VO} = 4000°K$ and $T = 1000°K$. Three different values of K are presented, K = 29 (Figures 8 and 9), K = 17 (Figure 10) and K = 10 (Figure 11). A comparison of Figures 4 and 8 shows that the 30 level model behaves very similarly to the lower 30 levels of the low temperature case up to maximum energy distribution. In Figure 8, this distribution is shown by the $t' = 6.72 \times 10^{-4}$ curve. However, there is no peaking in the inversion until after a time corresponding to V-V equilibrium is reached as described previously. The V-V quasisteady equilibrium distribution shown by the dashed line is calculated as before and the distribution shown at time $t' = 3.32 \times 10^{-3}$ is that distribution where $\bar{V}$ is equal to $\bar{V}$ at $t' = 0.0$. Note here that using 30 levels for the Treanor V-V equilibrium results in poor agreement between the two curves where $\bar{V}$ equals a constant. The reason for this is that

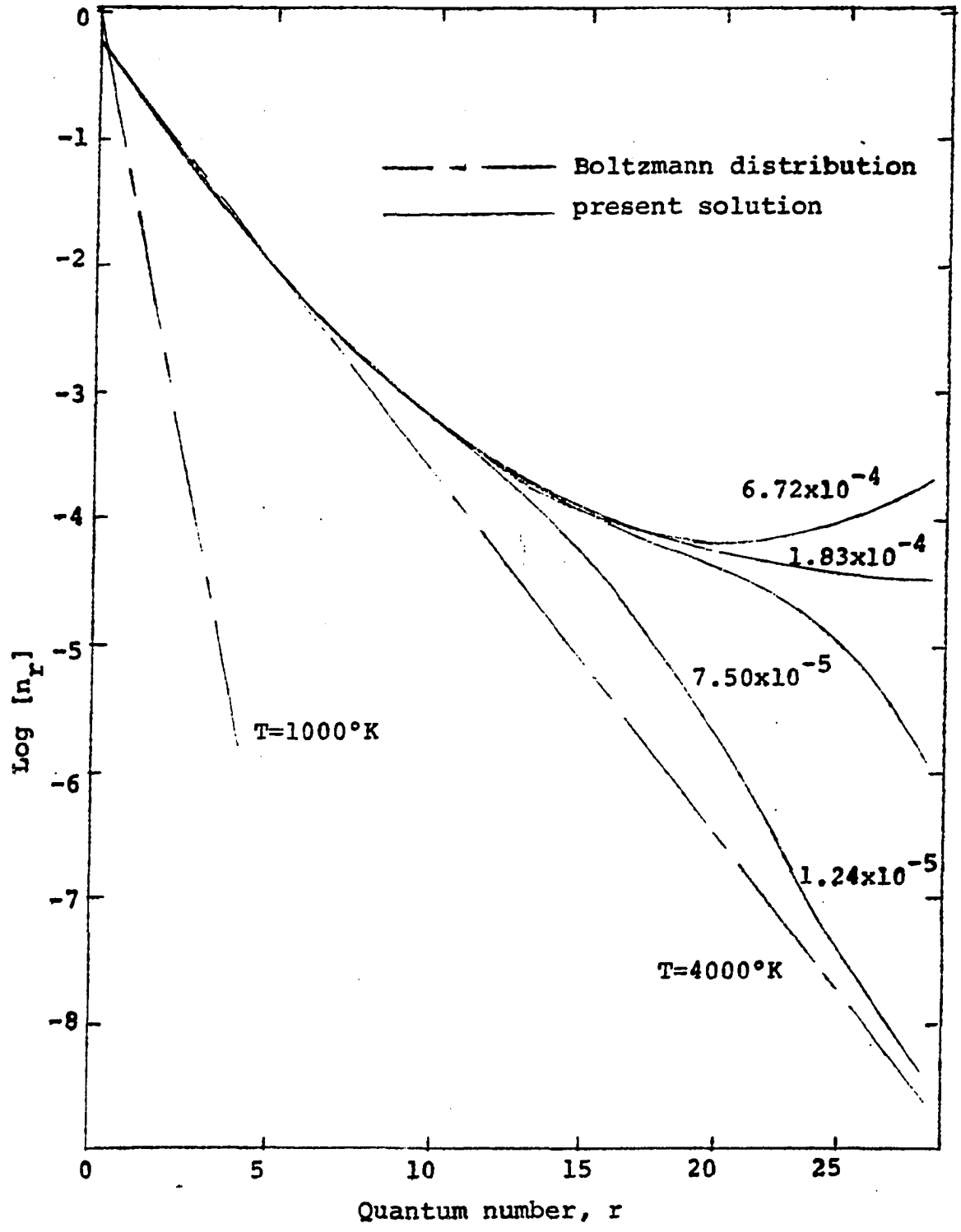

Figure 8. Population distribution for T_V=4000°K, T=1000°K and K=29 with $t'=nP_{10}t$ as the parameter

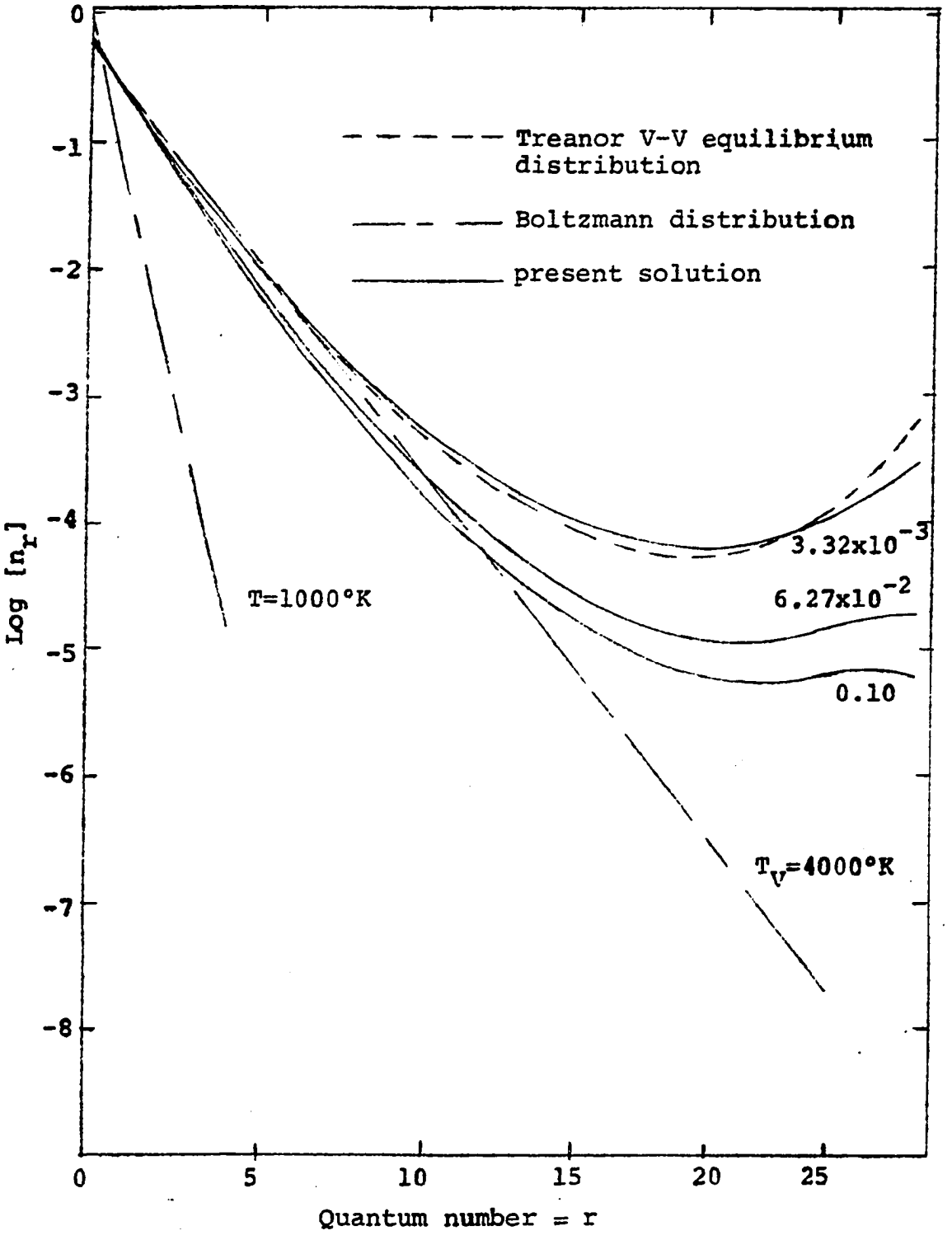

Figure 9. Population distribution for T_V=4000°K, T=1000°K and K=29 with $t'=nP_{10}t$ as the parameter. A Treanor V-V quasisteady distribution is shown for a 30 level model

the validity of the Treanor method is violated. This 30 level model does show the effect of the faster V-T exchange rates in the upper levels for a distribution given at t' = 0.1 as shown by the "peaking" of the inversion. A more complete anharmonic model (i.e., K > 40) would probably show the same type of distributions as the 45 level model does for the low temperature case.

Figures 10 and 11 exhibit behavior similar to that of Figure 7. That is, the distributions which correspond to Treanor V-V equilibrium are coincident with the Treanor V-V equilibrium distributions. Primarily, the reason for these lower level curves was to check the validity of the numerical technique used. For V-V dominated models, the complete master relaxation equations solutions should agree with the Treanor solution, and as can be concluded by Figures 7, 10 and 11, this is certainly true for the early stages of relaxation.

Vibrational Energy Distributions

Figures 12 and 13 are graphs of the nondimensional vibrational energy defined by Equation 3.2 versus non-dimensional time corresponding to the two temperature cases studied. The vertical marks pointing to a given curve represent the point in time for which the average number of vibrational quanta is equal to the initial value corresponding to that particular case. Again, this is V-V quasisteady

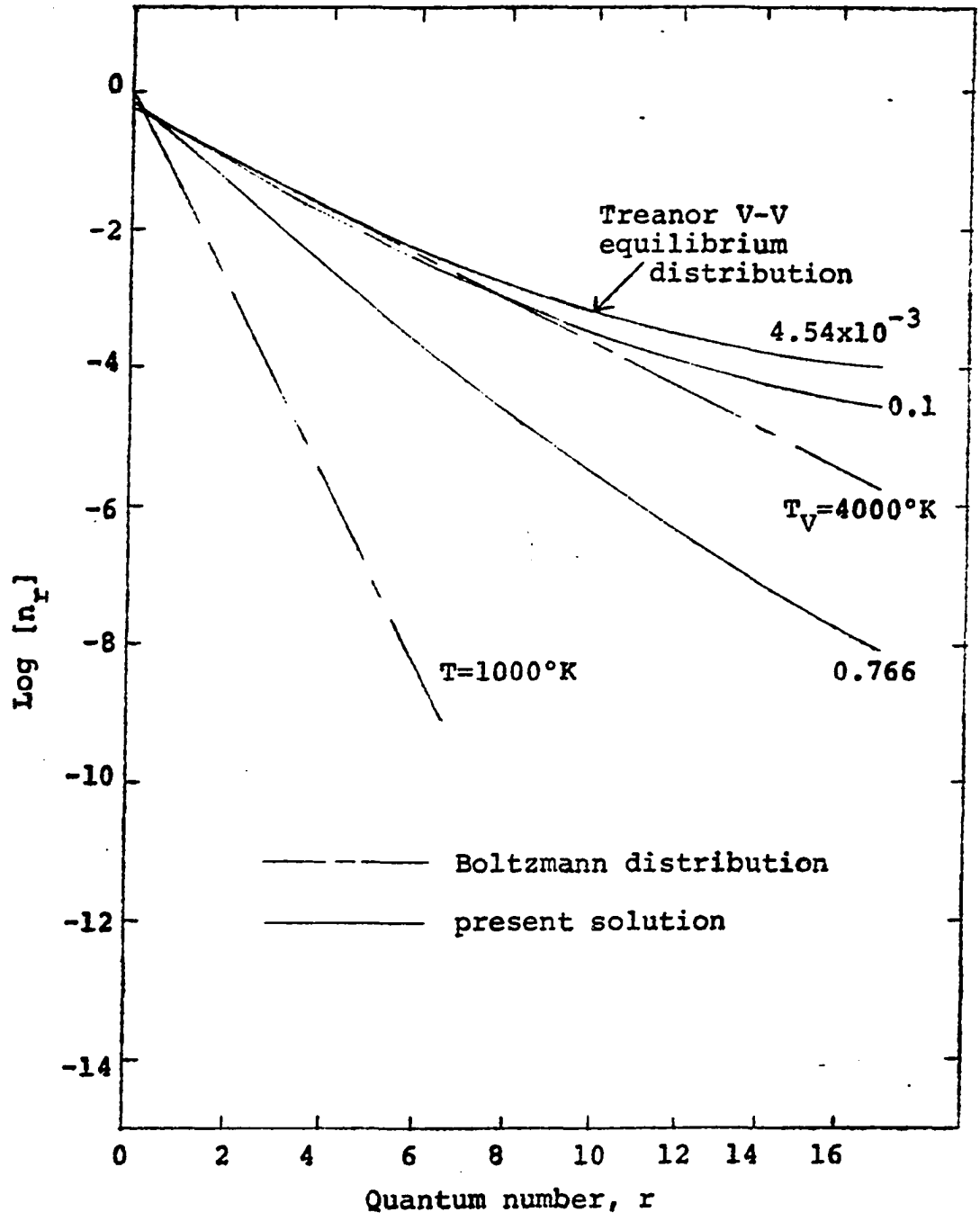

Figure 10. Population distribution for T_V=4000°K, T=1000°K and K=17 with $t'=nP_{10}t$ as the parameter

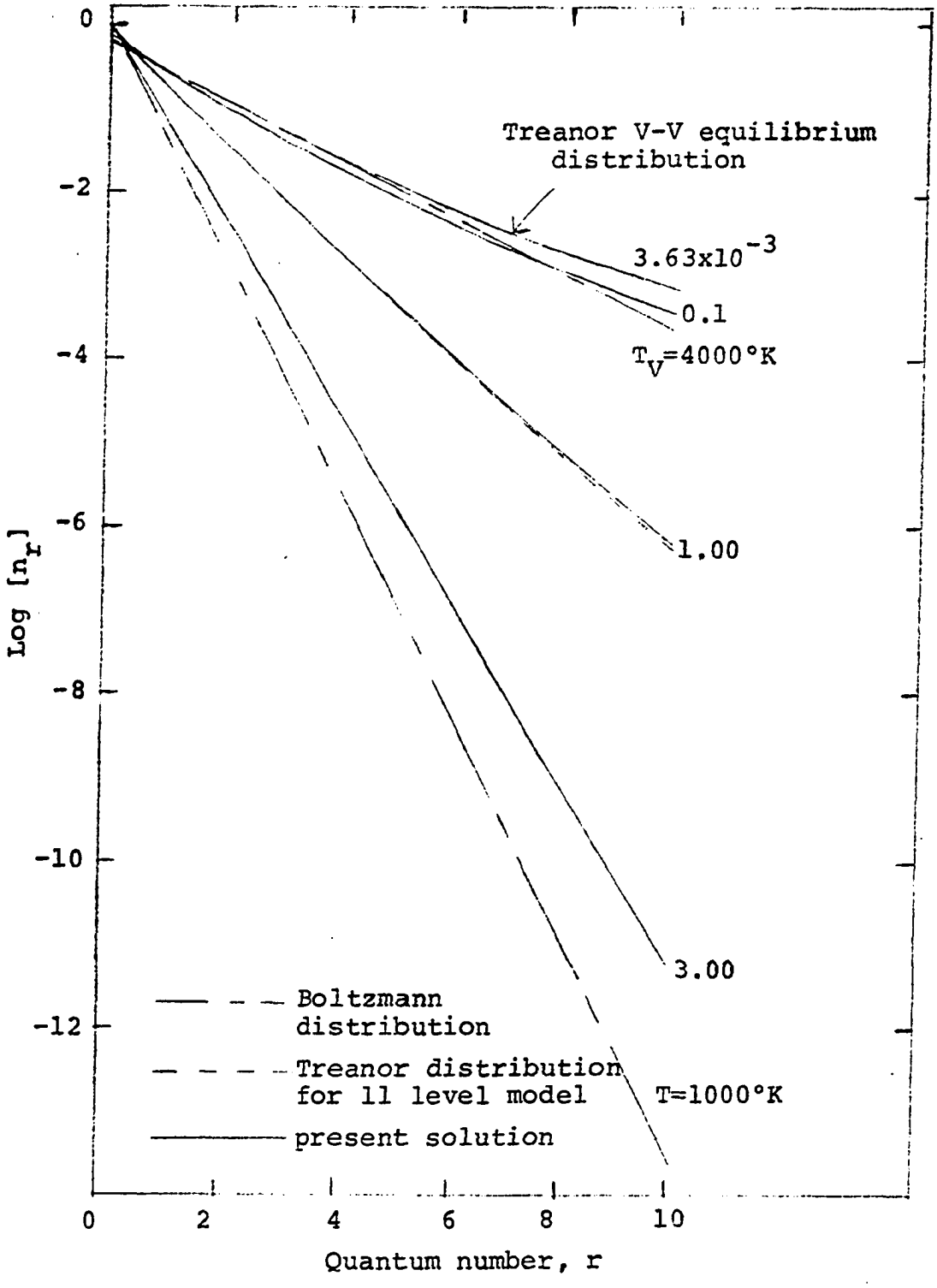

Figure 11. Population distribution for T_V=4000°K, T=1000°K and K=10 with $t'=nP_{10}t$ as the parameter. Also shown are Treanor distributions for an 11 level model

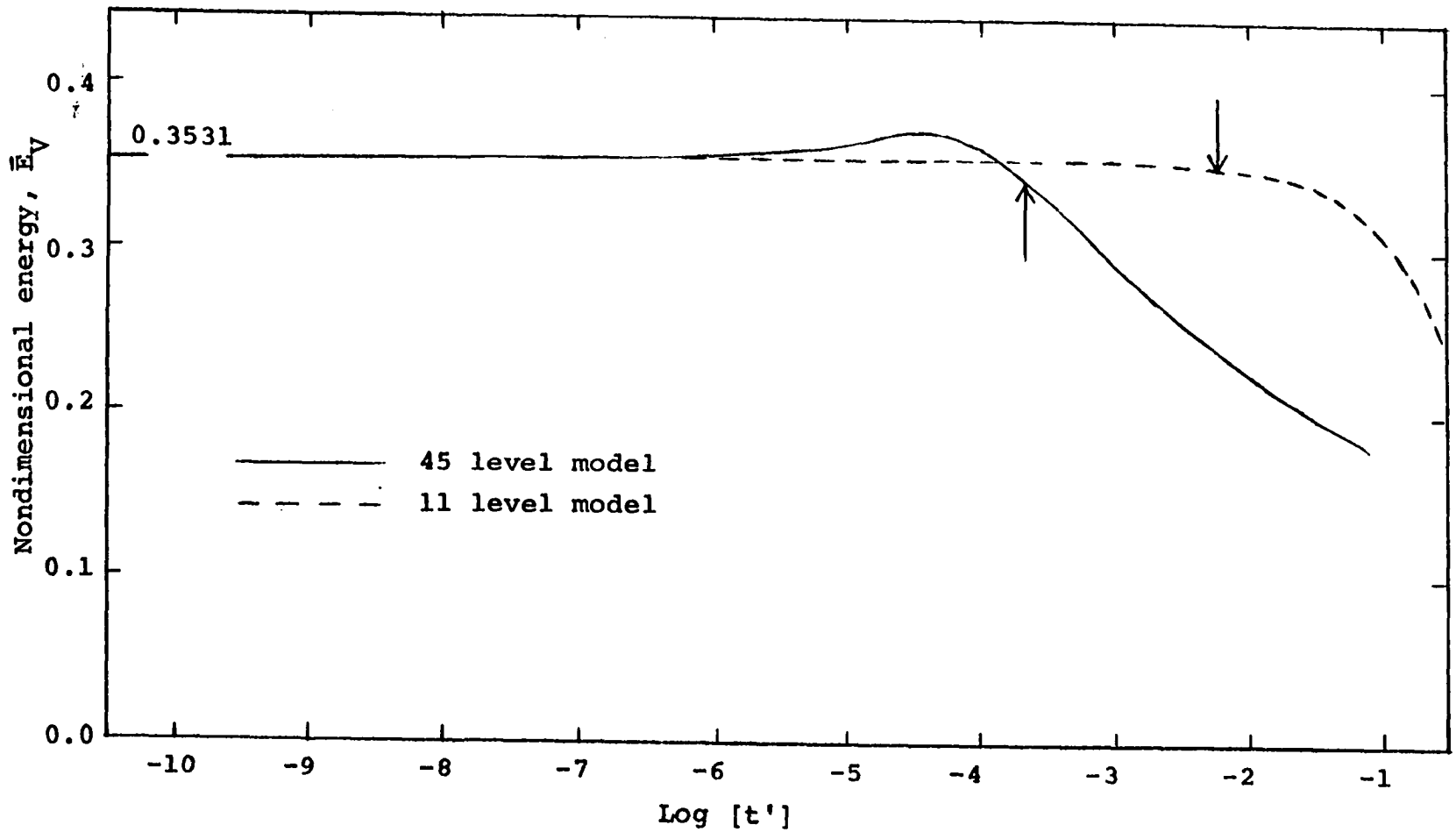

Figure 12. Variation of $\bar{E}_V=\Sigma_r rE_r/h\nu$ with respect to $t'=nP_{10}t$ for $T_V=2500°$ and $T=500°K$ using 45 and 11 level models. Initial value of E_V is also shown. Time marks indicate quasisteady state

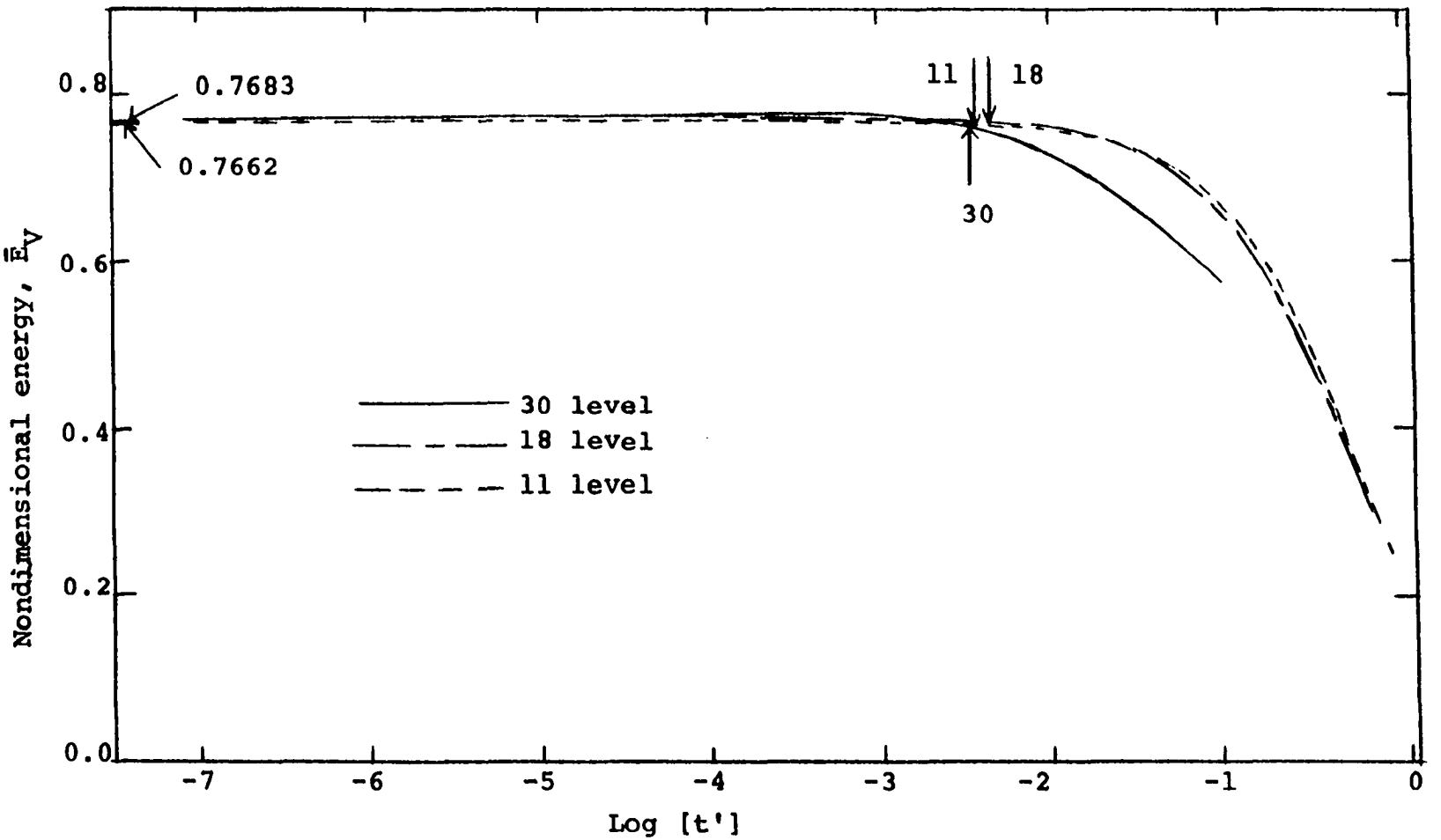

Figure 13. Variation of $\tilde{E}_V=\Sigma_r Er/h\nu$ with respect to $t'=nP_{10}t$ for T_V=4000°K and T=1000°K using 30, 18 and 11 level models. Initial value of E_V is shown. Time marks indicate quasisteady state

equilibrium in terminology. This particular time is often referred to in the text as V-V quasiequilibrium. These marks are labeled in Figure 13 according to the number of quantum levels used since they appear so close together. It is to be remembered that for the present investigation no quasisteady state exists in the sense defined by Treanor et al. (46) for the upper level models because no time scale separation can be justified for the complete models. In all cases the vibrational energy at the time flags or marks is less than it was when equilibrium existed at initial T_V. The decrease is always less than 3%. Between t' = 0.0 and the defined V-V quasisteady state, there is always an increase in dimensionless vibrational energy and average number of vibrational quanta. Table 3 shows the value of $\bar{E}_{Vmax}$ and the nondimensional time at which a maximum occurs.

This increase in vibrational quanta is not consistent with remarks made previously by others (6, 11, 17, 46) that during the establishment of an initial V-V equilibrium distribution there is no increase or decrease in vibrational quanta. As stated by these authors, the reason for the decrease in vibrational energy at V-V quasiequilibrium is because there is a shift of quanta to the upper levels.

It is found in this analysis that for an expansion flow process the V-V and V-T exchange processes interact to cause an increase in energy and vibrational quanta in the earliest

Table 3. Maximum $\bar{E}_V$ for the various cases investigated

T_V	Levels	$\bar{E}_{V_{max}}$	t'
2500	45	0.3724	3.979×10^{-5}
2500	11	0.3554	2.710×10^{-7}
4000	30	0.7743	6.716×10^{-4}
4000	18	0.7718	6.947×10^{-5}
4000	11	0.7689	2.322×10^{-5}

stages of relaxation. It will be remembered that V-V exchange processes have an exchange of vibrational energy with the translational mode. Because $\bar{E}_V$ and $\bar{V}$ both increase it shows that V-T exchange processes are involved in the early stages. In Figure 12 (low temperature case), the "bump" in the dimensionless energy curve does not occur until the upper 20 vibrational levels become significantly populated.

Relaxation Rate Expressions

In theoretical studies (5-7, 17, 46) it has been the practice to calculate vibrational "temperature" variation or the vibrational energy variation and compare that with the Landau-Teller rate since this is the theory that is used to reduce most experimental data where "temperatures" of given levels are usually measured. These vibrational temperatures are actually populating factors for a given level.

For example, Figures 14 and 15 show the comparison between the relaxation rate for the vibrational "temperature" of the $1 \rightarrow 0$ transition defined by

$$n_1 = n_o \exp - \left(\frac{E_1 - E_o}{k\theta_1^*} \right) \tag{3.4}$$

and that of the relaxation rate of the vibrational temperature of the Landau-Teller (20) model. This comparison is presented by plotting ψ_1 versus t' where

$$\psi_1 = d\theta_1^*/dt' / \left. \frac{d\theta_1^*}{dt'} \right)_{L.T.} \tag{3.5}$$

where $\left. d\theta_1^*/dt' \right)_{L.T.}$ is calculated according to the following expression (6):

$$\left. \frac{d\theta_1^*}{dt'} \right)_{L.T.} = - \frac{\theta_1^{*2}}{\frac{h\nu}{k}} (1 - \exp(-h\nu/kT))(1-\exp(h\nu/k\theta_1^* - \frac{h}{kT})) \tag{3.6}$$

where θ_1^* is obtained from Equation 3.4.

The derivative $d\theta_1^*/dt'$ is calculated from the slope existing in a θ_1^* versus t' distribution to the order of the stepsize squared (i.e., a parabola fit is used). The curves in Figures 14 and 15 are shown as drawn through symbols to indicate that the derivative calculation is not exact.

In Figure 14, the 45 level model differs radically from the 11 level model in the nondimensional time regime from

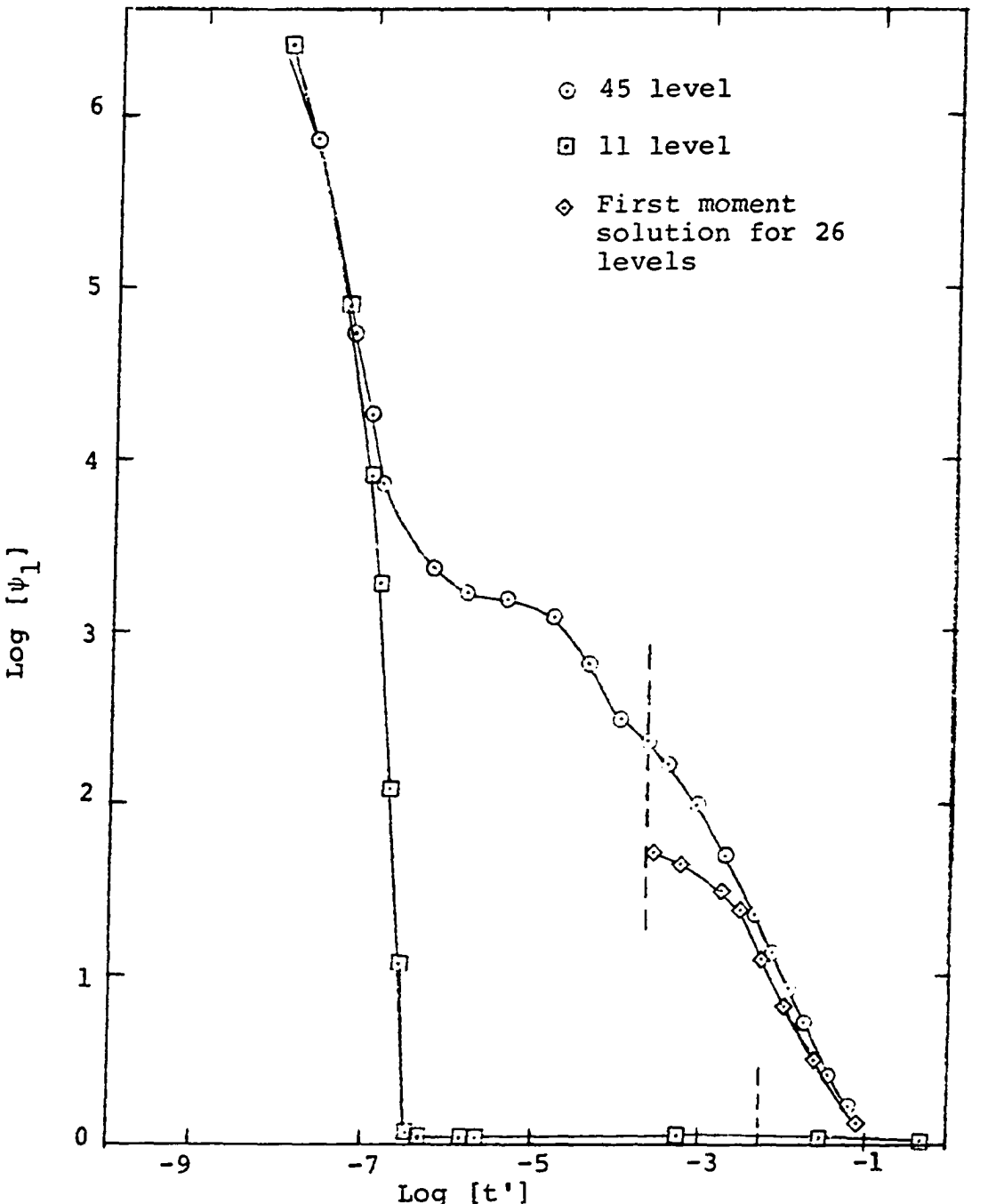

Figure 14. Distribution of de-excitation ratio, $\psi_1=(d\theta_1^*/dt')/(d\theta_1^*/dt')_{L.T.}$ with respect to $t'=nP_{10}t$ for $T_V=2500°K$, $T=500°K$ and 45 and 11 level models. De-excitation ratio using 1st moment solution is also shown beginning near the quasisteady state

2.0×10^{-7} to 2.0×10^{-2}. In the small time regime ($t' < 10^{-7}$) the 11 level and 45 level models give similar results for the rate of change of the vibrational "temperature" θ_1^*. This reflects that at the very earliest stages of relaxation the V-V exchange processes of the lowest levels rapidly redistributes the vibrational quanta toward a Treanor distribution. The deviation in the two curves is a result of the appearance of upper level population effects because of the anharmonicity of the model and the build up of the plateau in the population distributions. For a time corresponding to the previously defined V-V quasisteady equilibrium the ψ_1 value is 233, that is, at this time the relaxation rate of the first vibrational level temperature is 233 times faster than the Landau-Teller rate. At the corresponding V-V quasisteady equilibrium time for the 11 level model is equal to 1.17, that is, very little enhancement for this particular case. For this low level case the enhancement of the de-excitation rate is due only to the rapid readjustment of these levels into a Treanor distribution. At a value of t' slightly less than 0.1 the 11 level and 45 level mode results again agree very closely indicating once again the importance of anharmonicity in the early stages of relaxation ($t' < 10^{-1}$).

Included in Figure 14 is a curve showing the ψ_1 value for a 26 level first moment solution of the Treanor zeroth order solution in a manner described by Reference 17. The values

are plotted on the time scale assuming V-V quasiequilibrium for the Treanor solution occurs at $t' = 2.12 \times 10^{-4}$. Agreement between the two curves is close at values corresponding to $t' = 3.0 \times 10^{-3}$ but differ by a factor of 4 at t' values close to V-V quasiequilibrium. Therefore at times not too far from V-V quasiequilibrium, Treanor et al. (46) results give accurate temperature relaxation rates.

Similar results for the high temperature case are shown in Figure 15. On the basis of the trends shown in Figure 15 it can be reasonably conjectured that a model with more levels than 30 would exhibit a ψ_1 versus t' curve above that for the 30 level curve. Since the main difference between the low level models and high level models is that V-T effects are a factor to be considered in the higher models, it is reasonable to conclude that the high V-T probabilities give rise to a high de-excitation at the early stages of relaxation. It is certainly obvious that for times less than those corresponding to $t' = 0.1$ that measurement of relaxation at different times could give radically different results for ψ_1.

In Figure 16 is shown the value of ψ_7 for the low temperature case. This value is calculated according to the previous formulas given for ψ_1 except the subscript is replaced by 7. The interesting point to be made is that for values of $t' > 10^{-6}$ ψ_1 and ψ_7 agree very closely indicating the same relaxation behavior for these two "temperatures".

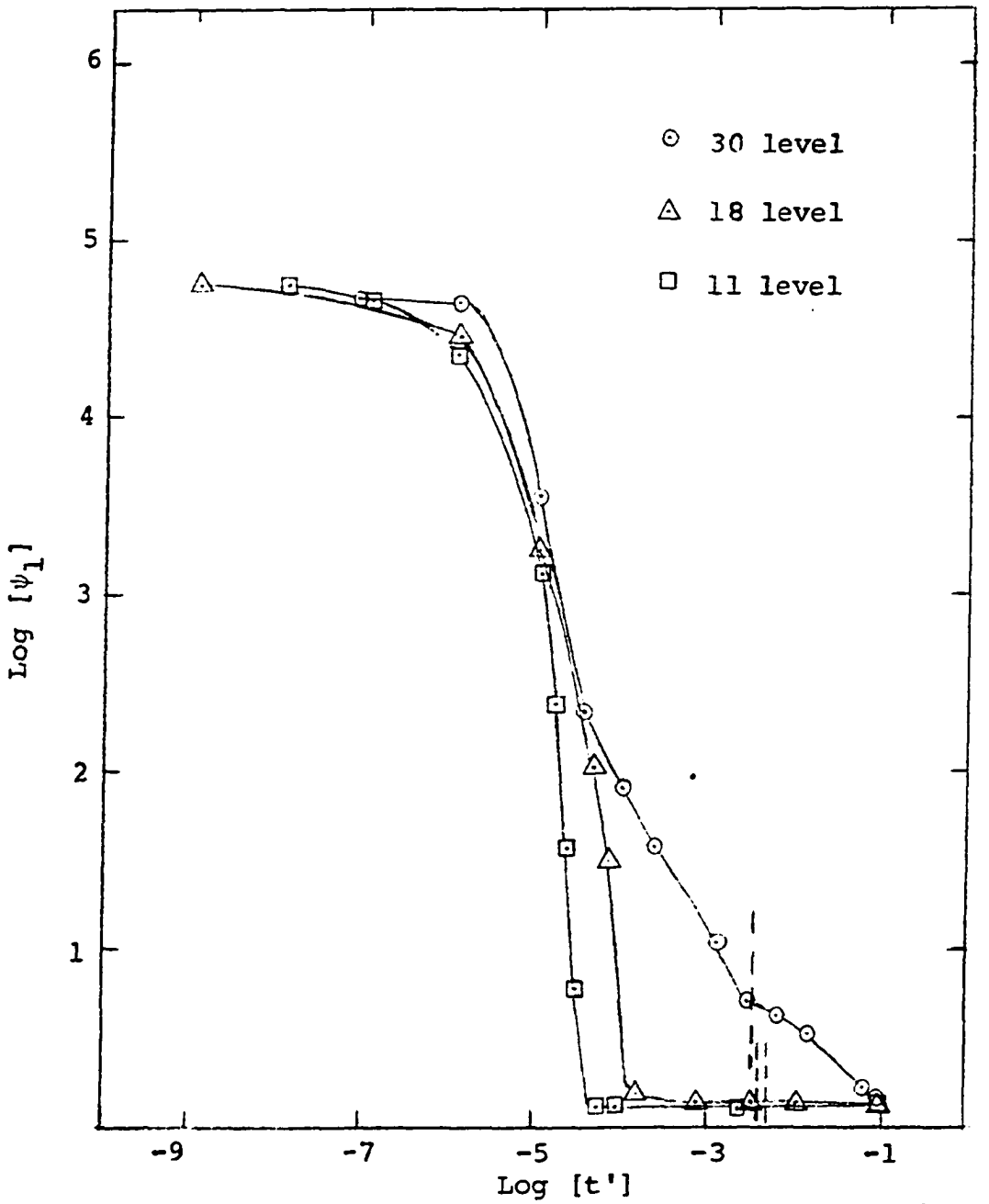

Figure 15. Distribution of de-excitation ratio, $\psi_1=(d\theta_1^*/dt')/(d\theta_1^*/dt')_{L.T.}$ with respect to $t'=nP_{10}t$ for T_V= 4000°K, T=1000°K and 30, 18 and 11 level models. Vertical dashed lines denote quasisteady state

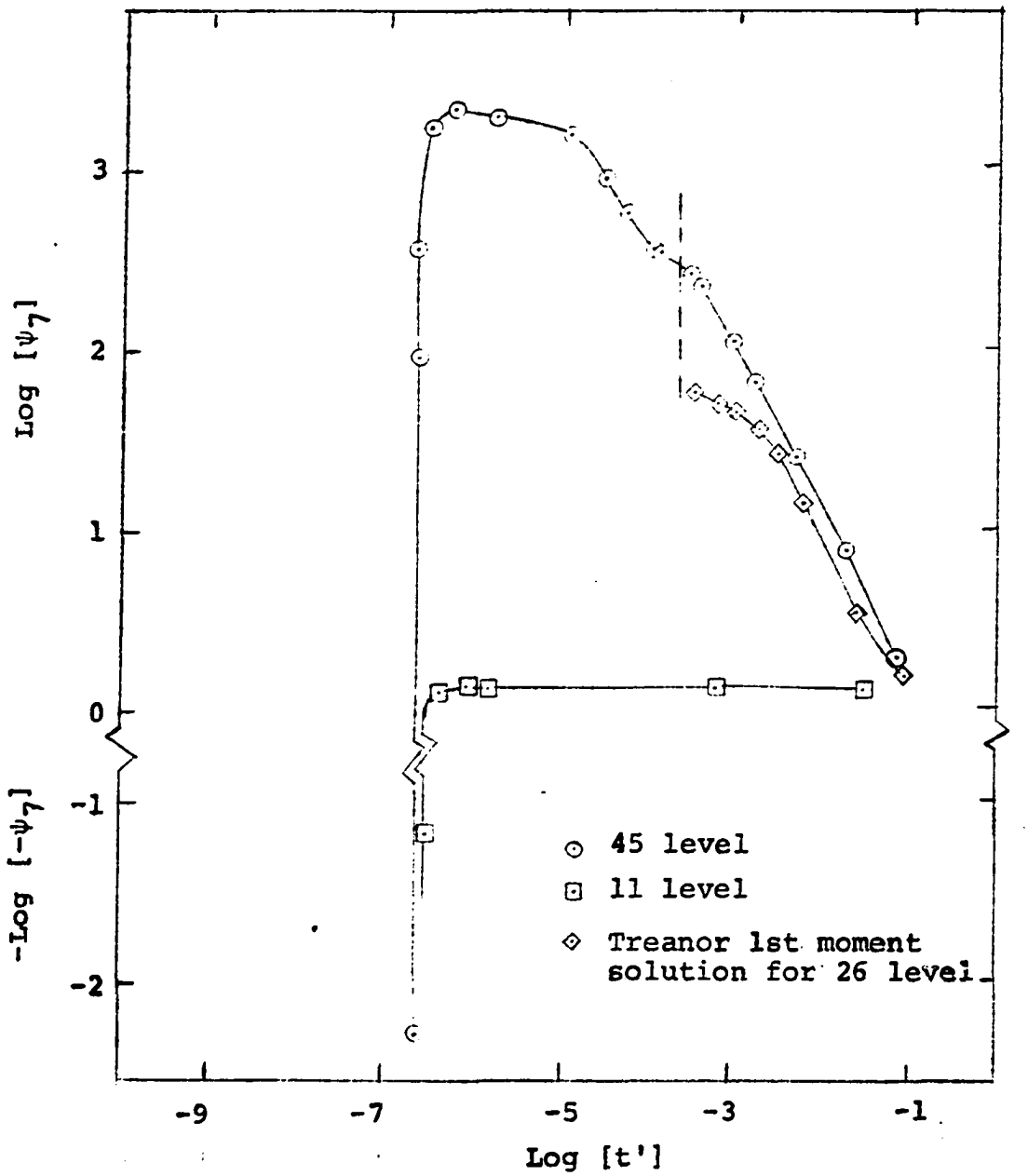

Figure 16. Distribution of de-excitation ratio, $\psi_7=(d\theta_7^*/dt')/(d\theta_7^*/dt')_{L.T.}$ with respect to $t'=nP_{10}t$ for $T_V=2500°K$, $T=500°K$ and 45 and 11 level models. De-excitation ratio using 1st moment solution is also shown beginning near quasisteady state

This is also the behavior of the vibrational level temperatures as shown in Figure 17. Because θ_7^* increases in value initially the value of ψ_7 will be negative until the maximum value is reached. Again, this early time behavior reflects the rapid readjustment of the lower levels into a Treanor distribution. Also shown is the Treanor first moment solution for the 7th level temperature variation. Again, this solution and the more complete solution have strong agreement at t' values greater than 3.0×10^{-3}.

Another relaxation rate parameter that is calculated for anharmonic oscillators is relaxation time based on vibrational energy (17) relaxation and then this relaxation rate parameter is compared to that for simple harmonic oscillator theory, i.e., with the τ of the Bethe-Teller equation (Equation 1.1). This ratio is defined as

$$\phi = \tau_{sho}/\tau_{aho} \tag{3.7}$$

where

$$\tau_{aho} = P_{10}n \; d(\ell n \; R)/dt' \tag{3.8}$$

where aho is an acronym for anharmonic oscillators and R is the reduced vibrational energy defined as

$$R = \frac{\bar{E}_V(\infty)-\bar{E}_V(0)}{\bar{E}_V(\infty)-E_V(t')} \tag{3.9}$$

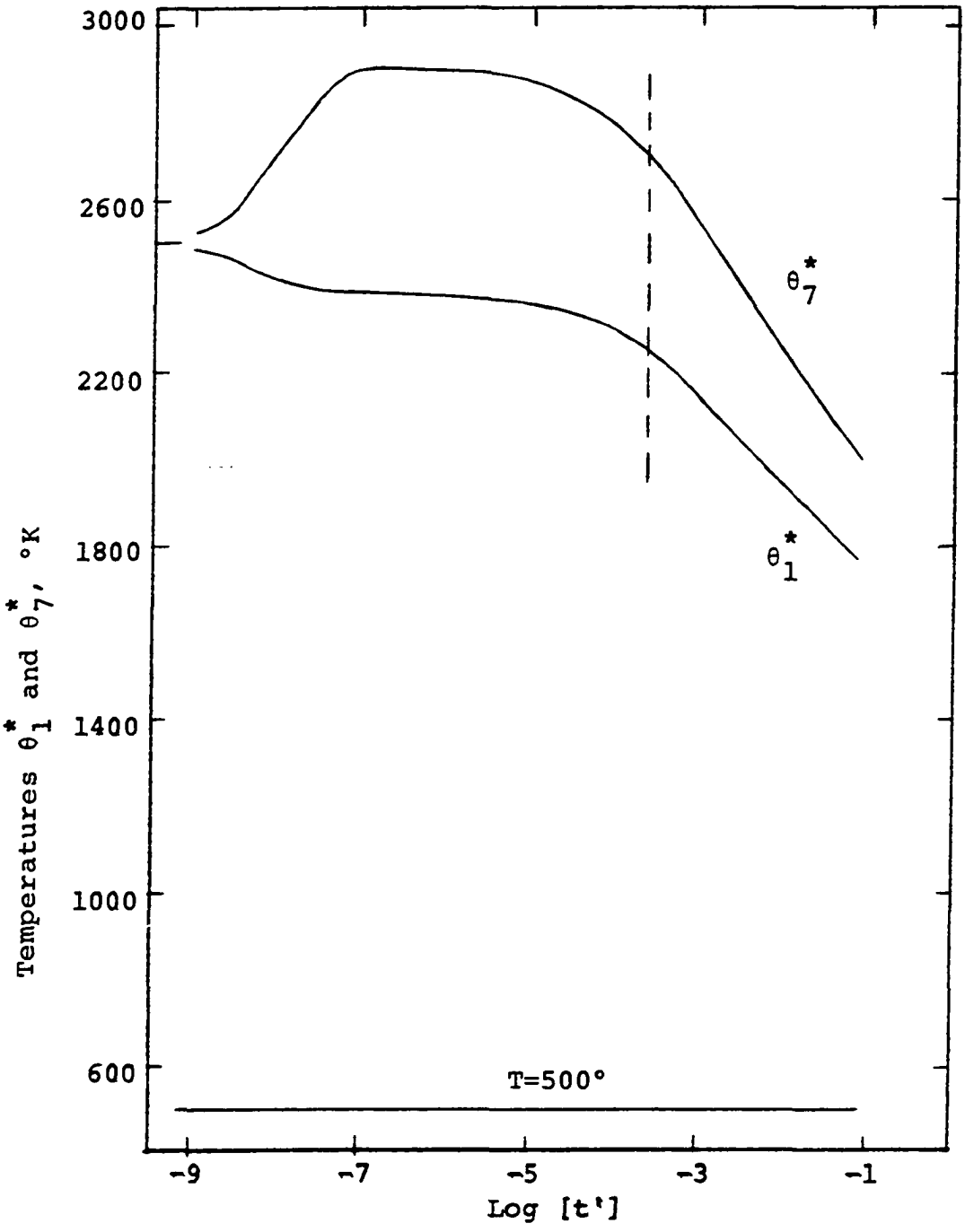

Figure 17. Variation of first and seventh population factors with respect to $t'=nP_{10}t$. Dashed vertical line indicates V-V quasisteady state

From Equation 3.7 it can be said that τ_{aho} is a local relaxation time. For harmonic oscillators, τ_{sho} is given by

$$\tau_{sho} = \frac{1}{P_{10}n(1 - \exp(-E_1/kT))} \qquad (3.10)$$

which is a constant for the cases studied because of the isothermal condition placed on the heat bath.

Figure 18 is a graph showing the variation of ϕ for $T_V = 2500°K$ and $T = 500°K$. A value for ϕ of greater than one indicates an energy relaxation rate for the anharmonic oscillator model exceeding that of the harmonic oscillator. The shape of the curve labeled 45 levels reflects the energy variation shown in Figure 12. On the basis of the above definitions, the relaxation rate actually becomes negative reflecting the increase in vibrational energy above its initial value. Again, Figure 18 shows large variations in ϕ occurring in very short time period. For the high temperature case the enhancement is not nearly as great in the 30 level model as for the 45 level model of the low temperature case (see Figure 18 and 19). This is another indication that the V-T exchange processes and anharmonicity are to be considered in a de-excitation flow process. Note that there is relatively little enhancement with the use of low level models based on an order of magnitude comparison for time $t' = 10^{-4}$ or greater.

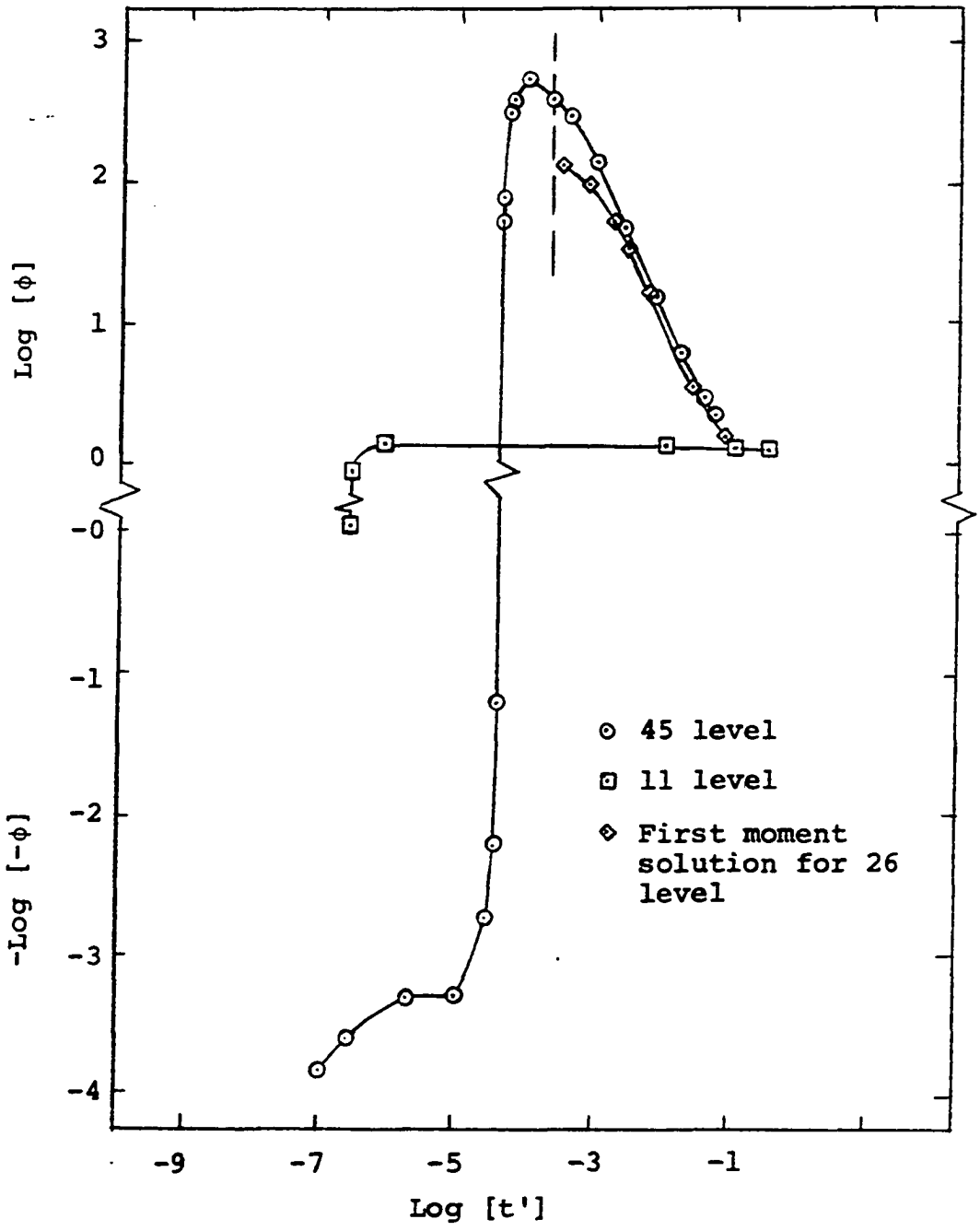

Figure 18. Variation of vibrational energy de-excitation ratio, $\phi=\tau_{sho}/\tau_{aho}$ with respect to $t'=nP_{10}t$ for T_V=2500°K, T=500°K and 45 and 11 level models. Also shown is ϕ variation from 1st moment solution

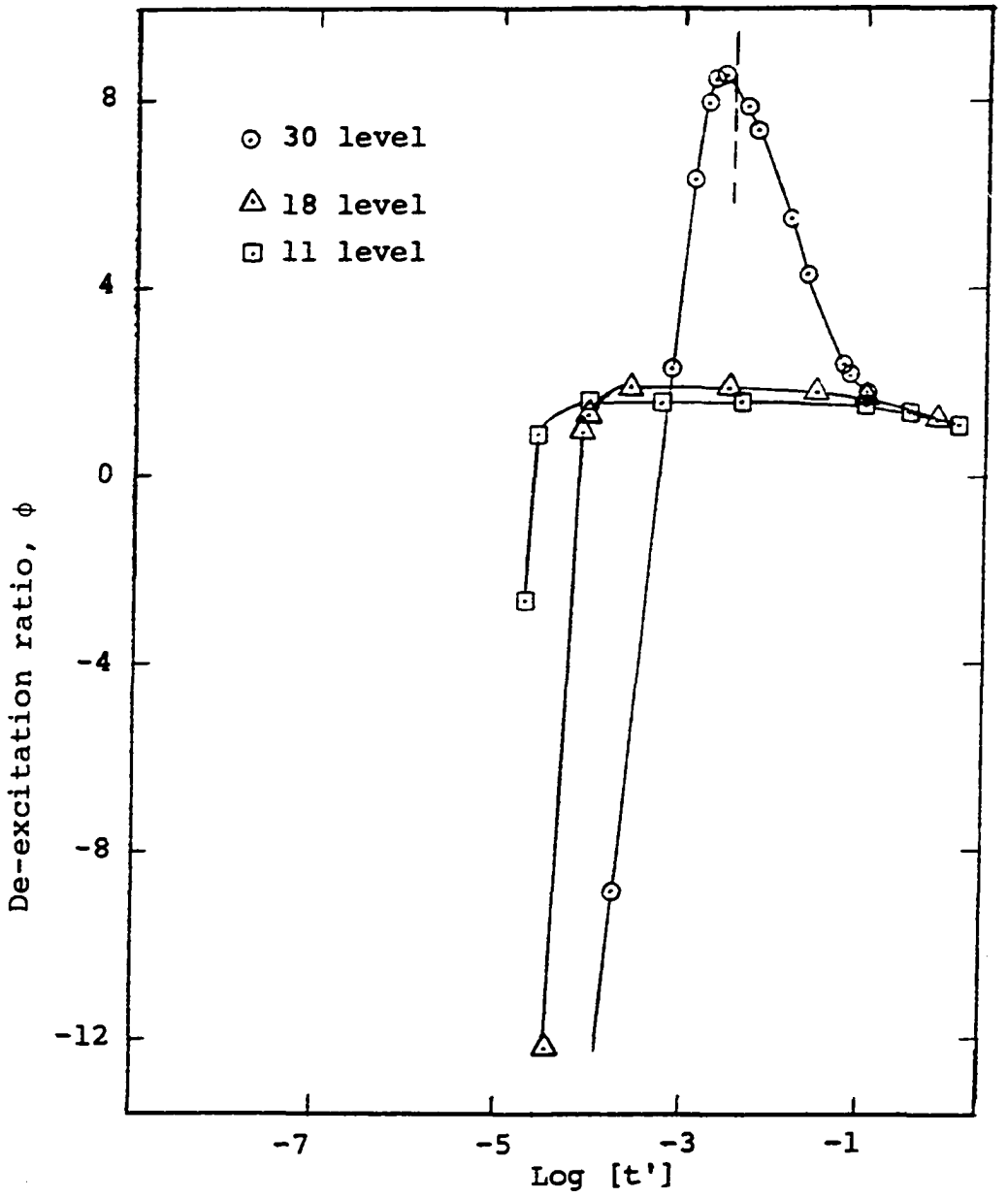

Figure 19. Variation of vibrational energy de-excitation ratio, $\phi=\tau_{sho}/\tau_{aho}$ with respect to $t'=nP_{10}t$ for T_V=4000°K, T=1000°K and 30, 18 and 11 level models. Dashed line indicates quasisteady state

Also shown in Figure 18 are values of ϕ using the Treanor method of solution. Again, results similar to temperature relaxation are noted.

In all relaxation cases studied an enhancement of the de-excitation rate was noted and at certain times this enhancement was very large with the largest variation in the values of ψ_1, ψ_7 and ϕ in the early stages of relaxation. But on the basis of this study there is very little difference between the relaxation rates for anharmonic oscillators and harmonic oscillators for values greater than $t' > 0.1$. Also, it will be noted that relaxation rates for the Treanor model differ from the present model only at times close to V-V quasiequilibrium. Although relaxation rates are the same magnitude, the reader is cautioned to remember that population distributions and vibrational energy values can differ by appreciable amounts at corresponding time where the relaxation rates are similar.

Discussion of Numerical Calculations

Recall that the procedure used to calculate a given model was to use a combination of an explicit method and the implicit method outlined in Chapter II. As was stated earlier, the predictor - corrector method was limited to small stepsizes because of stability criteria. The implicit method given in algorithm form by Equation 2.32 was used throughout much of

the integration time scale. Because computational time was a primary consideration, the largest possible stepsize was desired. As was explained in Chapter II and in the References 22-25, the stepsize could be chosen to be consistent with the accuracy of the largest driving eigenvalue as long as the method is stable for all eigenvalues. The error as given previously is of $O[H^3]$ for the implicit method.

Truncation error estimation was not established to arrive at great significant digit accuracy, but rather with the intent of obtaining solutions which were realistic for the upper vibrational levels at times where these values are important. Numerical checks were made on the local truncation error by comparing solutions between two different stepsizes in a manner described in Reference 41. If the two solutions agree to a certain criteria then the given stepsize is used. This particular local error estimation is used for stepsize control in NODE.

As stated earlier, the fact that the lower level systems should agree with a Treanor solution is a good check on the method. Finally, the fact that the total fractional population must add up to be one is a good check on the numerical technique to make sure the total solution is within reasonable physical bounds, for example, for the 45 level case the total population summation was equal to one to at least 8 significant

digits from t' = 0.0 to t' = 1.0 x 10^{-2} and at least 7 significant digits for t' greater than 10^{-2}.

It was also stated earlier that theoretically the numerical truncation error was the order of H^3, however, it must be remembered that this is purely an ordering term because the truncation error term is not only dependent upon stepsize but the value of the largest driving eigenvalue and a derivative value in the interval of concern. An attempt was made to keep accuracy of the upper level population at a value of 10^{-8} from times coincident with Treanor V-V equilibrium to larger values. This may be conservative in the sense that for population values to have any significant influence on relaxation rates it is felt they must have a magnitude of greater than approximately 10^{-6}.

The implicit solutions shown in Figure 7 were achieved using a stepsize the $O[10^{-3}]$ with driving eigenvalues calculated to be of $O[10^{2}]$. To achieve similar accuracy i.e., solutions valid at 10^{-8}, for the 45 level case a stepsize of $O[10^{-4}]$ was used to arrive at the solutions shown in Figure 6 because the driving eigenvalues were of $O[10^{3}]$. In Figure 5, the implicit method was used with a stepsize of $O[10^{-7}]$. It must be noted here that the theory of truncation error and accuracy as discussed in References 22-25 disregards round off error which may or may not be a problem. Analysis of the calculated eigenvalues showed that the magnitude of the

driving eigenvalues decreased in magnitude as t' became larger. This should allow accuracy to improve for a given stepsize. No difficulty was encountered in the high temperature case because the calculated driving eigenvalue was always less than those for the low temperature case. Hence, a stepsize of $O[10^{-3}]$ presented no difficulties. Because the lower level models predicted Treanor first moment results, the worthiness of the implicit method is strengthened when applied to the larger level cases.

First Order Solutions

As stated earlier in Chapter II, an attempt was made to solve the first order solution of the Treanor et al. (46) theory in order to determine what this correction was. This first order solution is given by the solving of Equation 2.20 which are a set of linear algebraic equations in Φ's. Use of two different techniques were used to solve this set of equations for different level systems. One method was a Gaussian elimination technique which gave values of Φ the order of 10^{15} to 10^{16}, and the other technique involved the matrix inversion of the coefficients of Φ. This latter technique gave values close to 10^{7} - 10^{8}. All these values are unrealistic in the sense that their use would result in fractional population values of greater than 1 (see Equation 2.18). Numerically, the difficulty was a result of "ill-

conditioning" of the matrix. What the cause of the "ill-conditioning" was was never determined because the same results were achieved for systems involving 5, 11, 16 and 26 level systems. There may be a similarity between this problem and that of the parasitic and driving eigenvalue structure of the linearized master relaxation equations. Furthermore, it may be a problem associated with the particular temperature used (in cases studied T_V = 2500°K and 500°K were used) because as was noted above the eigenvalue structure in terms of magnitude was different for the two temperature cases.

For the large level cases it may be expected to have problems because the ordering process does not reduce all transition probabilities to the same order as can be noted by the curves shown in Figure 1. That is division by ε into the upper V-T transition probabilities will cause these values to exceed V-V transition probabilities by a minimum of 10^5. This certainly is not consistent with the premise of the ordering procedure outlined in Chapter II which states that after division by ε the V-T and V-V transition rates are of the same order. However, for a 5 level system the ordering should be correct but the same "ill-conditioning" results as for the large system even when double precision arithmetic was used.

CHAPTER IV. CONCLUDING REMARKS

Conclusions

The vibrational relaxation of diatomic nitrogen gas initial at high vibrational energy immersed in a constant low temperature heat bath to simulate an expansion flow was analyzed by numerically integrating the complete set of master relaxation equations. The temperature ratio between the initial equilibrium temperature and final equilibrium temperature was 4 or 5. A number of conclusions can be drawn from the investigation of vibrational energy de-excitation using the complete set of master relaxation equations using various number of vibrational quantum levels.

1. The population distributions of the diatomic oscillators is definitely a non-Boltzmann distribution in the early stages of relaxation. The earliest stages of relaxation involve rapid readjustment of the lower quantum levels into a Treanor distribution as a result of the V-V exchange processes. The intermediate quantum level distribution of oscillators approach a plateau very quickly and then as time proceeds show a more characteristic inversion distribution. The upper most quantum level populations of the anharmonic oscillator are constantly trying to be maintained in a distribution approaching a Boltzmann distribution of the heat bath temperature.

2. A full or nearly full level model is important in determining accurate de-excitation rates in the early stages

of relaxation of vibrational energy de-excitation. However, at times corresponding to the secular adjustment period of Treanor et al. (46), the differences between the large level models, small level models and a Treanor V-V model results are small indicating that the lowest quantum levels are the most important in determining relaxation behavior rates.

3. The relaxation rates vary by a considerable amount over the short period of time in the early stages of relaxation. The ratio of first level temperature relaxation for the complete model divided by Landau-Teller temperature relaxation for the cases where high vibrational energy exists in a low temperature environment was very high initially and approached the Landau-Teller rate in a very short time. Vibrational energy de-excitation rates show this same behavior of widely varying relaxation rates in the early stages of the deexcitation problem. These results indicate that orders of magnitude of difference could exist in measured experimental relaxation rates depending on the time such measurements are taken.

4. A method for integrating the "stiff" master relaxation equations was used and proved to be quite successful.

5. The Treanor model used previously by Treanor et al. (46) and Hsu and Maillie (17) who did a time variation of the Treanor first moment method gives good results in most of the time regime where it can be applied and is only inaccurate in the time corresponding to initial V-V equilibrium, where it

underestimates the relaxation rates by approximately a factor of 4.

6. The results of Bray (6) near the quasisteady equilibrium where he calculated population distribution and a first level temperature relaxation rate for a given set of conditions near this quasisteady state are found to be qualitatively correct. That is, the population distribution form is similar to those shown by him and the relaxation rate enhancement near quasiequilibrium requires vibration level temperature of a high magnitude in comparison with the heat bath temperature. How accurate his (6) results are in comparison to the total time history of relaxation cannot be determined because his reported results are based on calculations where θ_1^* is given and assumed to exists at some point near the above defined quasisteady state.

Recommendations for Further Research

In light of the work reported in this dissertation, several suggestions or recommendations can be made that would be of interest to study.

1. One of the obvious extensions would be to calculate the 45 or full level model for the T_V = 4000°K and T = 1000°K case using the above technique. From the author's experience with the method used on the two temperature cases, this high temperature case should require less computation time than was

needed for the low temperature case.

2. Incorporation of a nonisothermal heat bath condition would yield results that would be quite helpful.

3. Calculation of relaxation rates for other gases, notably carbon monoxide, would be of benefit since most experimental data of vibrational energy de-excitation is done using carbon monoxide.

4. Further research in the calculation of transition probabilities especially at high quantum levels and using two or three dimensional collisions would result in more physically exact results.

5. Further research in the area of integrating "stiff" equations would be of benefit to work dealing with vibrational energy relaxation where the use of master relaxation equations are important. Also, a more detailed analysis of the eigenvalue structure maybe would allow some improvement in the above method.

6. Finally, a variable stepsize control maybe developed for the above method on the basis of the changes in the vibrational population values and the accuracy desired similar to a technique suggested by Lomax and Bailey (25). A method using a change of stepsize criteria based on population level values for the 11 level model for T_V = 4000°K and T = 1000°K

was tried for a short time period with good results although not enough data was obtained for conclusive comparisons. And certainly continued research in the area of error analysis is of obvious value.

CITED REFERENCES

1. Bazely, N. W., Montroll, E. W., Rubin, R. J. and Shuler, K. E. Studies in nonequilibrium rate processes. III. The vibrational relaxation of a system of anharmonic oscillators. J. Chem. Phys. 28: 700-704. 1958.

2. Bethe, H. A. and Teller, E. Deviations from thermal equilibrium in shock waves. Aberdeen Proving Ground, Md., Ballistic Research Laboratory Report X-117. 1941.

3. Blom, A. P., Bray, K. N. C. and Pratt, N. H. Rapid vibrational de-excitation influenced by gasdynamic coupling. Revised version of the paper presented at 2nd International Colloquium on Gasdynamics of Explosions and Reactive Systems, Novosikirsk. 1969.

4. Bray, K. N. C. Chemical and vibrational nonequilibrium in nozzle flows. In Wagener, P. P., ed. Nonequilibrium flows. Part II. Pp. 59-157. New York, New York, Marcel Dekker, Inc. 1970.

5. Bray, K. N. C. Vibrational relaxation of anharmonic oscillator molecules. M.I.T. Fluid Mech. Lab. Pub. No. 67-3. 1967.

6. Bray, K. N. C. Vibrational relaxation of anharmonic oscillator molecules: relaxation under isothermal conditions. J. Phys. B 1: 705-717. 1968.

7. Bray, K. N. C. Vibrational relaxation of anharmonic oscillator molecules: II. Non-isothermal conditions. J. Phys. B 3: 1515-1538. 1970.

8. Clarke, J. F. and McChesney, M. The dynamics of real gases. Washington, D.C., Butterworth, Inc. 1964.

9. Cottrell, T. L. and McCoubrey, J. C. Molecular energy transfer in gases. London, England, Butterworths and Co. Ltd. 1961.

10. Crane, R. L. Stability and local accuracy of numerical methods for ordinary differential equations. Unpublished Ph.D. thesis. Ames, Iowa, Library, Iowa State University. 1962.

11. Fisher, E. R. and Kummler, H. Relaxation by vibration-vibration exchange processes. Part I. Pure gas case. J. Chem. Phys. 49: 1075-1084. 1968.

12. Gerry, E. T. Gasdynamic lasers. AIAA Paper No. 71-23. 1971.

13. Hertzberg, A., Johnston, E. W. and Ahlstrom, H. G. Photon generators and engines for laser power transmission. AIAA Paper No. 71-106. 1971.

14. Herzfeld, K. F. and Litovitz, T. A. Absorption and dispersion of ultrasonic waves. New York, New York, Academic Press. 1959.

15. Hsu, C. T. and McMillen, L. D. On the first moment relaxation equation of anharmonic oscillators. J. Chem. Phys. 53: 4107-4108. 1970.

16. Hsu, C. T. and Maillie, F. H. Reply to comments by Bray and Pratt. J. Chem. Phys. 53: 2988-2989. 1970.

17. Hsu, C. T. and Maillie, F. H. Vibrational relaxation of anharmonic oscillators with vibration-vibration and vibration-translation energy exchanges. J. Chem. Phys. 52: 1767-1772. 1970.

18. Hurle, I. R. and Russo, A. L. Spectrum-line reversal measurements of free electron and coupled N_2 vibrational temperatures in expansion flows. J. Chem. Phys. 43: 4434-4443. 1965.

19. Hurle, I. R., Russo, A. L. and Hall, J. G. Spectroscopic studies of vibrational nonequilibrium in supersonic nozzle flows. J. Chem. Phys. 40: 2076-2089. 1964.

20. Landau, V. L. and Teller, E. Zur theorie der schalldispersion. Physik. Z. Sowjetunion 10: 34-43. 1936.

21. Lapidus, L. and Seinfeld, J. H. Numerical solution of ordinary differential equations. New York, New York, Academic Press, Inc. 1971.

22. Lomax, H. An operational unification of finite difference methods for the numerical integration of ordinary differential equations. NASA TR R-262. 1967.

23. Lomax, H. On the construction of highly stable, explicit, numerical methods for integrating coupled ordinary differential equations with parasitic eigenvalues. NASA TN D-4547. 1968.

24. Lomax, H. Stable implicit and explicit numerical methods for integrating quasi-linear differential equations with parasitic-stiff and parasitic-saddle eigenvalues. NASA TN D-4703. 1968.

25. Lomax, H. and Bailey, H. E. A critical analysis of various numerical integration methods for computing the flow of gas in chemical nonequilibrium. NASA TN D-4109. 1967.

26. Magnus, D. E. and Schechter, H. S. Analysis of error growth and stability for the numerical integration of the equations of chemical kinetics. General Applied Science Laboratories, Inc. Technical Report 607. 1966.

27. Maillie, F. H. Vibrational relaxation of anharmonic oscillators with vibration-vibration and vibration-translation energy exchange. Unpublished Ph.D. thesis. Ames, Iowa, Library, Iowa State University. 1969.

28. Montroll, E. W. and Shuler, K. E. Studies in non-equilibrium distributions. I. Collisional relaxation of a system of harmonic oscillators. J. Chem. Phys. 25: 59-67. 1956.

29. Moretti, G. A new technique for the numerical analysis of nonequilibrium flows. AIAA Journal 3: 223-229. 1965.

30. Northrup, L. L. and Hsu, C. T. Vibrational energy relaxation with multiple quantum transitions. Phys. of Fluids 11: 1376-1377. 1968.

31. Osipov, A. E. The relaxation of the vibrational motion in an isolated system of harmonic oscillators. Soviet Physics-Doklady 5: 102-104. 1960.

32. Osipov, A. I. and Stupochenko, E. V. Nonequilibrium energy distributions over the vibrational degrees of freedom in gases. Soviet Physics-Uspekhi 6: 47-66. 1963.

33. Rankin, C. C. and Light, J. C. Relaxation of a gas of harmonic oscillators. J. Chem. Phys. 46: 1305-1316. 1967.

34. Rapp, D. and Englander-Golden, P. Resonant and near-resonant vibrational-vibrational energy transfer between molecules in collision. J. Chem. Phys. 40: 573-575. 1964.

35. Rapp, D. and Kassal, T. The theory of vibrational energy transfer between simple molecules in non-reactive collisions. Chemical Reviews 69: 61-102. 1969.

36. Rich, J. W. and Rehm, R. G. Vibrational relaxation of anharmonic oscillators. Cornell Aeronautical Laboratory Report AF-2022-A-2. 1967.

37. Rubin, R. J. and Shuler, K. E. Relaxation of vibrational nonequilibrium distributions. I. Collisional relaxation of a system of harmonic oscillators. J. Chem. Phys. 25: 59-67. 1956.

38. Rubin, R. J. and Shuler, K. E. Relaxation of vibrational nonequilibrium distributions. II. The effect of the collisional transition probabilities on the relaxation behavior. J. Chem. Phys. 25: 68-74. 1956.

39. Russo, A. L. Importance of impurities on vibrational relaxation measurements in N_2. J. Chem. Phys. 44: 1305-1306. 1966.

40. Schwartz, R. N., Slawsky, Z. I. and Herzfeld, K. F. Calculation of vibrational relaxation times in gases. J. Chem. Phys. 20: 1591-1599. 1952.

41. Seinfeld, J. H., Lapidus, L. and Hwang, M. Review of numerical integration techniques for stiff ordinary differential equations. Industrial Engineering and Chemical Fundamentals 9: 266-275. 1970.

42. Sharp, T. E. and Rapp, D. Evaluation of approximations used in the calculations of excitation by collision. II. Vibrational excitation of molecules. J. Chem. Phys. 43: 1233-1244. 1965.

43. Shuler, K. E. Relaxation of an isolated ensemble of harmonic oscillators. J. Chem. Phys. 32: 1692-1697. 1960.

44. Tannehill, J. C. and Anderson, E. W. Intermediate altitude rocket exhaust plumes. AIAA J. of Spacecraft and Rockets (to be published).

45. Treanor, C. E. Molecular vibrational energy distributions during exchange dominated relaxation. Cornell Aeronautical Laboratory Report AF-2184-A-1. 1966.

46. Treanor, C. E., Rich, J. W. and Rehm, R. G. Vibrational relaxation of anharmonic oscillators with exchange dominated collisions. J. Chem. Phys. 48: 1798-1807. 1968.

47. Tyson, T. J. An implicit integration method for chemical kinetics. TRW Space Technology Laboratories Report 9840-6002-RV000. 1964.

48. Vincenti, W. G. and Kruger, C. H., Jr. Introduction to physical gas dynamics. New York, New York, John Wiley and Sons, Inc. 1965.

49. von Rosenburg, C. W., Jr., Taylor, R. L. and Teare, J. D. Vibrational relaxation of CO in nonequilibrium nozzle flow. J. Chem. Phys. 48: 5731-5733. 1968.

50. von Rosenburg, C. W., Jr., Taylor, R. L. and Teare, J. D. Vibrational relaxation of CO in nonequilibrium nozzle flow, and the effect of hydrogen atoms on CO relaxation. J. Chem. Phys. 54: 1974-1988. 1971.

ACKNOWLEDGEMENTS

It is with sincere gratitude that the author acknowledges Dr. C. T. Hsu for his advice and guidance in the conduction of this research and for his counseling throughout the author's graduate studies.

The author would like to thank the other members of his committee for their cooperation and helpfulness: Prof. R. C. Fellinger, co-chairman, Dr. W. J. Cook, Dr. J. D. Iversen and Dr. R. H. Homer; to the Engineering Research Institute for partial financial support of computer time; to the National Science Foundation for financial support; to Mrs. Maxine Bogue for the typing of the manuscript.

The author also wishes to express special thanks to his wife Rose for her sacrifices and support throughout his graduate program.

APPENDIX

The objective of this appendix is to show the equivalence between two algorithms given below:

$$[I - \frac{1}{2} H A_i] \underline{n}_{i+1} = \underline{n}_i + \frac{1}{2} H f_i \tag{A-1}$$

$$[I - \frac{1}{2} H A_i] \underline{n}_{i+1} = [I - \frac{1}{2} H A_i] \underline{n}_i + H \underline{F}_i + O(H^3) \tag{A-2}$$

Equation A-1 is the algorithm given by Equation 2.32 and A-2 is that method given in References 22-25 for integrating a system of stiff equations. The right hand side of Equation A-1 and Equation A-2 can be shown to be equivalent if the quantity $H \underline{F}_i$ is added and subtracted to Equation A-2 and some algebraic manipulation is performed.

To show that $\frac{1}{2} H \underline{f}_i - H \underline{F}_i + H \underline{F}_i$ can be written as $-\frac{1}{2} H[A_i]n_i + H \underline{F}_i$ consider the following set of quasilinear O.D.E.'s

$$W_1' = F_1 = aw_1 + bw_2 + cw_1w_2 \tag{A-3}$$

$$W_2' = F_2 = dw_1 + ew_2 + fw_1w_2$$

In matrix notation Equations A-3 become

$$\underline{w} = \underline{F}(\underline{w}) \tag{A-4}$$

Equations A-3 represent the general form of the quasilinear master relaxation equations. Now, as in Chapter II, $\underline{f}_i$

represents the linear terms of Equations A-3 at a representative step i, therefore $\frac{1}{2}$ H $\underline{f}_i$ - HF_i becomes

$$\begin{bmatrix} -\frac{1}{2} Haw_{1_i} & -\frac{1}{2}Hbw_{2_i} & -\frac{1}{2}H(cw_{1_i}w_{2_i} + cw_{1_i}w_{2_i}) \\ -\frac{1}{2}Hdw_{1_i} & -\frac{1}{2}Hew_{2_i} & -\frac{1}{2}H(fw_{1_i}w_{2_i} + fw_{1_i}w_{2_i}) \end{bmatrix} \qquad \text{(A-5)}$$

a column vector, which can be rewritten as

$$-\frac{1}{2}H \begin{bmatrix} a + cw_{2_i} & b + cw_{1_i} \\ d + fw_{2_i} & e + fw_{1_i} \end{bmatrix} \begin{bmatrix} w_{1_i} \\ w_{2_i} \end{bmatrix} \qquad \text{(A-6a)}$$

or

$$-\frac{1}{2}H[A_i]\underline{w}_i \qquad \text{(A-6b)}$$

where in Equation A-6b, $[A_i]$ is the Jacobian of Equations A-3. Therefore the equivalency between Equation A-1 and A-2 is shown which means that Equation A-1 is accurate to $O[H^3]$.